



**Michigan  
Technological  
University**

Michigan Technological University  
**Digital Commons @ Michigan Tech**

---

Dissertations, Master's Theses and Master's Reports

---

2015

## **ANALYSIS OF NO<sub>2</sub> AND HCHO VERTICAL COLUMN DENSITIES IN THE GREAT LAKES REGION USING THE OZONE MONITORING INSTRUMENT**

David J. Faber

*Michigan Technological University, [djfaber@mtu.edu](mailto:djfaber@mtu.edu)*

Copyright 2015 David J. Faber


---

### **Recommended Citation**

Faber, David J., "ANALYSIS OF NO<sub>2</sub> AND HCHO VERTICAL COLUMN DENSITIES IN THE GREAT LAKES REGION USING THE OZONE MONITORING INSTRUMENT", Open Access Master's Report, Michigan Technological University, 2015.

<https://doi.org/10.37099/mtu.dc.etdr/37>

Follow this and additional works at: <https://digitalcommons.mtu.edu/etdr>

 Part of the [Atmospheric Sciences Commons](#)

**ANALYSIS OF NO<sub>2</sub> AND HCHO VERTICAL COLUMN DENSITIES  
IN THE GREAT LAKES REGION USING THE OZONE  
MONITORING INSTRUMENT**

By

David J. Faber

A REPORT

Submitted in partial fulfillment of the requirements for the degree of

MASTER OF SCIENCE

In Geology

MICHIGAN TECHNOLOGICAL UNIVERSITY

2015

©2015 David J. Faber



This report has been approved in partial fulfillment of the requirements for the Degree of  
MASTER OF SCIENCE in Geology.

Department of Geological and Mining Engineering and Sciences

Report Advisor: *Louisa Kramer*

Committee Member: *Paul Doskey*

Committee Member: *Claudio Mazzoleni*

Committee Member: *Simon Carn*

Department Chair: *John Gierke*



*This work is dedicated to my wife and family.  
I couldn't have made this journey without them.*



## Table of Contents

Abstract .....	8
1. Introduction .....	9
1.1 Motivation .....	9
1.2 O <sub>3</sub> Production by NO <sub>x</sub> and VOCs .....	14
1.3 State of Research .....	17
1.3.1 OMI Retrieval Campaigns .....	17
1.3.2 Formaldehyde-to-NO <sub>2</sub> Ratio .....	18
1.4 Objectives and Hypotheses .....	18
1.5 Outline of Thesis .....	20
2. Methodology .....	20
2.1 Data Collection .....	20
2.2 Error Analysis .....	24
2.3 Data Processing .....	25
3. Results .....	26
3.1 Comparison to Ground-Based Instruments .....	26
3.2 Gradient from Chicago to the Keweenaw Peninsula .....	31
3.3 Gradient from Detroit to Mackinac Bridge .....	45
3.4 Seasonal Dependence of FNR .....	58
4. Discussion .....	59
4.1 Sensitivity Analysis .....	59
4.2 NO <sub>2</sub> Gradients .....	60
4.3 HCHO Gradients .....	61
4.4 FNR Gradients .....	62
5. Conclusion .....	64
List of References .....	67



## **Abstract**

Nitrogen oxides ( $\text{NO}_x$ ) and volatile organic compounds (VOC) are major contributors to air quality, especially for their direct involvement in ozone ( $\text{O}_3$ ) production. Retrievals of nitrogen dioxide ( $\text{NO}_2$ ) and formaldehyde (HCHO) mixing ratios can be used to represent  $\text{NO}_x$  and VOCs respectively and the formaldehyde-to- $\text{NO}_2$  ratio (FNR) can be used to analyze the  $\text{O}_3$  production chemistry in a region. Since the current monitoring network in the Great Lakes region for  $\text{NO}_2$  and HCHO is limited, the Ozone Monitoring Instrument (OMI) can be used to retrieve vertical column densities for  $\text{NO}_2$  and HCHO in rural areas away from ground-based sensors. OMI was found to be sensitive to temporal changes in ground mixing ratios and suitable for this study. OMI was able to retrieve statistically significant gradients for  $\text{NO}_2$  and FNR but not HCHO between urban centers and rural areas in the Great Lakes region. Data from OMI was used to determine regions of VOC-limited  $\text{O}_3$  production and  $\text{NO}_x$ -limited  $\text{O}_3$  production. FNR values are highest in rural areas and during the summer months.

# 1. Introduction

## 1.1 Motivation

Anthropogenic nitrogen oxide ( $\text{NO}_x = \text{NO} + \text{NO}_2$ ) sources are significant contributors to the overall composition and chemistry of the atmosphere. Measurement of these sources will lead to understanding of how emitted gases impact atmospheric chemistry and future climate. Point sources, such as power plants and major industrial facilities and large-scale sources such as cities are major contributors to pollution, injecting large amounts of  $\text{NO}_x$  into the local atmosphere. Highways, with their automobile traffic, are near continuous sources of  $\text{NO}_2$  as well, albeit from a linear path rather than a point source. Highway emissions vary with traffic conditions as heavier traffic will result in higher emissions. Due to wind, traffic, surface boundary layer height and turbulent motion highway sources can be treated as being within several hundred meters of the highway [Durant et al. 2010]. Small towns can also be micro-sources of  $\text{NO}_2$ ; however limited measurements from small towns in rural areas have been performed. Shipping is also a major source of  $\text{NO}_x$  with gas emissions from the stacks of large ships. Shipping routes across the Great Lakes may potentially impact air quality in the surrounding region. Accurate measurements of all these gas sources may help the scientific community to evaluate changes in  $\text{NO}_x$  from sources. If existing understanding of gas sources is incorrect, model simulations will not reflect the reality of the atmosphere. Modeling of chemical reactions in the atmosphere, transport of emissions and changes in climate requires correct understanding of the gas sources and this understanding is not just of the largest sources but also the sum total of all the small sources in rural regions. Measurements across large regions will also aid policy making through improved pollution regulation and validate reports of emissions provided by industries to ensure that regulation is followed. Furthermore, establishing a more reliable way to measure sources in the future will be vital to a functioning atmospheric monitoring network.

Volatile organic compounds (VOC) such as formaldehyde ( $\text{HCHO}$ ), isoprene, and terpenes are emitted to the atmosphere from both natural and anthropogenic sources. The volatile nature and low boiling point of the compounds lead to sublimation and

evaporation from solid and liquid forms into the atmosphere. From there, VOCs can be transported within the atmosphere. The sources of VOCs are numerous in both urban areas and undeveloped rural areas and regions between. Major natural sources include emissions from plants and trees and major anthropogenic sources include industrial processes. In both urban and natural, VOCs may also be passively emitted from evaporation and sublimation. Measurement of total VOC content is challenging because of the variety of VOCs present in the atmosphere but measurement of one or two VOCs such as HCHO may be a functional analogue of total VOC content. As with NO<sub>x</sub>, measurements of VOCs across large regions will also aid policy making, pollution regulation, and validation of emission reports. Establishment of a more reliable way to measure VOCs will be vital to the monitoring network.

Emission inventories for both NO<sub>x</sub> and VOC are available from the EPA [EPA 2014]. Inventories from 2014 of both chemical families can be found in Table 1. Major sources for NO<sub>x</sub> include fuel combustion and vehicles on and off the highway. Major sources for VOC include the petroleum industry, solvent use, and miscellaneous sources.

Source Category	NO <sub>x</sub> (thousands of tons)	VOC (thousands of tons)
<b>FUEL COMB. ELEC. UTIL.</b>	1,776	41
<b>FUEL COMB. INDUSTRIAL</b>	1,258	112
<b>FUEL COMB. OTHER</b>	555	476
<b>CHEMICAL &amp; ALLIED PRODUCT MFG</b>	51	83
<b>METALS PROCESSING</b>	71	34
<b>PETROLEUM &amp; RELATED INDUSTRIES</b>	685	2,774
<b>OTHER INDUSTRIAL PROCESSES</b>	353	329
<b>SOLVENT UTILIZATION</b>	1	2,811
<b>STORAGE &amp; TRANSPORT</b>	20	1,043
<b>WASTE DISPOSAL &amp; RECYCLING</b>	83	132
<b>HIGHWAY VEHICLES</b>	4,489	2,159
<b>OFF-HIGHWAY</b>	2,669	1,845
<b>MISCELLANEOUS incl. WILDFIRES</b>	399	5,290
<b>Total</b>	12,412	17,130

Table 1: 2014 Emission Inventories for NO<sub>x</sub> and VOC divided by source category. [EPA 2014].

The transport of pollution adds another layer of complexity with regards to the impact of these gases downwind. Plumes of gases transported from distant sources can result in elevated levels in remote regions. Transport of  $\text{NO}_x$  from urban sources to rural areas may also lead to unexpected rises in tropospheric ozone ( $\text{O}_3$ ) as  $\text{NO}_x$  may react with VOCs from rural and wilderness sources such as forests.  $\text{O}_3$  production from the reaction of  $\text{NO}_x$  and VOCs occurs in either a  $\text{NO}_x$  limited or a VOC limited regime depending on which gas is in excess [Olszyna et al 1994].  $\text{O}_3$  production in rural areas, which have an excess of VOCs from vegetation and other sources is in a  $\text{NO}_x$  limited regime and highly responsive to small changes in  $\text{NO}_x$ . Studying these impacts is challenging due to the complex chemical reactions and dynamic processes occurring within the transported plumes.

Measurement and understanding of  $\text{NO}_x$ , VOC,  $\text{O}_3$ , and the chemistry surrounding these gases is important as all three are major pollutants and have potential health risks [Sandström 1995, Haagen-Smit 1952]. Tropospheric  $\text{O}_3$  can have a strong negative impact on health and it is a major component in smog.  $\text{NO}_x$  is a major contributor to acid rain and tropospheric  $\text{O}_3$  is a greenhouse gas. These gases can also be responsible for property damage and crop damage. Regulation and control of these gases are important for the well-being of the local population and the environment.

In addition to being an ozone precursor it has also been shown that  $\text{NO}_x$  emissions can affect aerosol particle nucleation and growth in the area near to the power plant which can have powerful effects on the atmosphere and climate [Lonsdale et al. 2012].

Measurement of highway sources is important since automobile traffic emissions are a significant contributor to local levels of pollutants such as  $\text{NO}_x$  [Redling et al. 2013; Singer et al. 2004]. Long range transported emissions may also contribute to the measurements made over highways. Satellite instruments can identify pollution sources along major routes but lack the spatial resolution to measure smaller highway emissions because of the large pixel size and infrequent transits.

Measuring a gradient from urban areas to rural areas will also help understand the impact of gas transport from urban to rural. Since urban areas have more sources of  $\text{NO}_2$  than rural areas, it is expected that a gradient of  $\text{NO}_2$  column density will be present.

However, transported gases from urban areas and micro-sources in the rural areas may alter the gradient from current expectations. Retrieval of this gradient will improve understanding of the impact of transported emissions on rural areas, especially with regards to the VOC-limited and  $\text{NO}_x$ -limited regimes of  $\text{O}_3$  production and the gradient between them.

In addition to emissions from power plants, highways, and industrial areas in the Great Lakes regions, emissions from shipping traffic on the Great Lakes and related waterways are an area of concern as ships are a source of  $\text{NO}_x$ . Shipping traffic in other parts of the world has been shown in several research studies to be a significant contributor to the overall emission budget of a region [McIntosh 2013; Kim et al. 2011; Dalsøren et al. 2013; Tzannatos 2010].

A recent study [McIntosh 2013] showed that shipping traffic through the Soo Locks may be a major contributor to emissions in the Great Lakes region. Therefore, retrievals of  $\text{NO}_2$  near ports will provide important information on the impact of ships on pollution near the shore of the Great Lakes and downwind.

Knowledge of VOCs from anthropogenic and natural sources are important for the study of the atmosphere and modeling of ozone production. The major issue with understanding and measuring the sources of VOCs is the diversity of species in the chemical family. VOCs include alkanes, alkenes, aromatics, aldehydes, ketones, carbonyls, ethers, and alcohols. Previous research has catalogued the variety of VOC species emitted from biological sources [Atkinson and Arey 2003]. VOCs react with  $\text{NO}_x$  to produce  $\text{O}_3$  but the reactivity of each VOC is different and so the  $\text{O}_3$  production resulting from each VOC is different [Carter 1994]. The sum total of individual production rates from each VOC will then be the total  $\text{O}_3$  production. Because of this, it is difficult to determine the total production from all VOC species; instead a usable substitution needs to be found. Retrieval of a single commonly found VOC such as HCHO may work as a substitution.

Measurements of  $\text{NO}_x$  and VOC in rural areas of the Great Lakes region are underrepresented in the literature. The Great Lakes region contains several major urban centers, smaller urban regions, small towns, and rural regions, both agricultural and

forested wilderness, all connected by a network of highways. The Great Lakes also hold a large amount of shipping traffic to and from ports on the lake coasts. Furthermore, the Great Lakes themselves account for a very high percentage of the world's freshwater lake area. Because of these features, the region is very diverse for study with large and small sources and the agricultural, freshwater, and wilderness resources could be in danger from pollution effects. Because much of this region is not covered by existing monitoring network assets, there may be pollution sources unaccounted for in the current understanding and modeling of the atmosphere in the region. Additionally, the transport of pollutants and reaction chemistry of the regions is unknown due to the lack of monitoring assets. It is unlikely that the rural regions of the Great Lakes region will be nonattainment areas – those areas with air quality worse than the National Ambient Air Quality Standards – but there may be better or worse air quality than can be expected given current assumption of the region.

Analysis during this study will focus in the western Great Lakes region in Michigan, Wisconsin, and Illinois. Currently the rural Great Lakes region has a very limited ground-based monitoring network for NO<sub>2</sub> and VOC. Sources expected in this region include fuel combustion for electricity and industry – as the region contains a great deal of industry and many of the power plants burn fuel – and highway emissions – as the region contains many highways and highway shipping. There is likely a great deal of off-highway vehicle emissions with recreational vehicles – such as powered watercraft and off-road vehicles – and industrial vehicles such as for logging and mining. As mentioned previously, shipping traffic on the Great Lakes themselves is a major source for pollution as well.

The goal of this research is to determine the effectiveness of the Ozone Monitoring Instrument (OMI) to evaluate the air quality in rural regions, through the retrieval of NO<sub>2</sub> and VOC vertical column densities. OMI is well documented as a tool for urban areas but current scientific literature is limited on OMI's ability to retrieve column densities in rural areas. Two obstacles stand in the way of retrievals in rural areas: inherent error in the instrumental technique and detection limits. In light of these obstacles, this research seeks to investigate the possibility of using OMI as a tool in rural air quality studies. Three main goals are present for this research. First, it must be determined whether OMI

retrievals are representative of changes in ground concentration for  $\text{NO}_2$  and  $\text{HCHO}$ . Second, OMI's ability to resolve significant gradients from urban to rural are investigated. Third, using the column densities of  $\text{NO}_2$  and  $\text{HCHO}$ , it will be determined if OMI can be used to study air quality and  $\text{O}_3$  production chemistry in the region including an investigation into  $\text{NO}_x$ -limited regime and VOC-limited regimes and where the chemistry shifts from one regime to another.

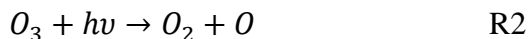
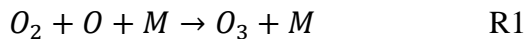
## 1.2 Atmospheric Chemistry of $\text{NO}_x$ , VOCs, and $\text{O}_3$

$\text{NO}_x$  is produced in the atmosphere from the reaction of diatomic oxygen ( $\text{O}_2$ ) and diatomic nitrogen ( $\text{N}_2$ ) at high temperatures. Both species are major components in the atmosphere and are functionally non-limited in the reaction. These high temperatures can be created by combustion reactions from anthropogenic sources such as power plants, vehicle engines, and industry or from natural sources such as wildfires. The intense heat from a stroke of lightning during a storm can also be a source for  $\text{NO}_x$ . Other chemical reactions can also lead to production of  $\text{NO}_x$  such as those from agricultural fertilization and nitrogen-fixing plants. Reaction between  $\text{NO}$  and  $\text{NO}_2$  is considered to be fast making the two species a chemical family; photolysis converts  $\text{NO}_2$  to  $\text{NO}$  and reaction with oxygen converts the  $\text{NO}$  back into  $\text{NO}_2$ .  $\text{NO}_x$  as a chemical family, however, has a lifetime of about a day with destruction pathways in day and night through oxidation to  $\text{HNO}_3$ ; this limits long-range transport unless  $\text{NO}_x$  is reacted to a reservoir species such as peroxyacetylnitrate (PAN).

$\text{HCHO}$  is produced through oxidation of other VOCs that are emitted from combustion events and industrial processes as well as natural sources. The exact pathways to  $\text{HCHO}$  are dependent on the specific precursor VOCs.  $\text{HCHO}$  is destroyed by either photolysis or reaction with  $\text{OH}$ . These destruction pathways cause  $\text{HCHO}$  to have a short atmospheric lifetime around a few hours. Long range transport of  $\text{HCHO}$ , and VOCs in general, is thus unlikely as the  $\text{HCHO}$  or VOC would be destroyed before it reaches its downwind destination.

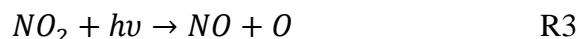
$\text{O}_3$  is produced in the atmosphere by reaction between  $\text{O}_2$  and free oxygen ( $\text{O}$ ).  $\text{O}_3$  is destroyed in a reaction with UV light to form  $\text{O}_2$  and  $\text{O}$ . These reactions form a cycle

with no loss, therefore O and O<sub>3</sub> sometimes get combined to form the odd-oxygen chemical family (O<sub>x</sub>=O+O<sub>3</sub>) since there is fast reaction between the two.

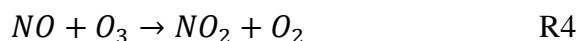


Since O<sub>2</sub> and UV light are virtually limitless for this equation during the day, the production of O<sub>x</sub> and therefore O<sub>3</sub> is based on the production of odd oxygen (O). There are many pathways and reactions to form O in the atmosphere but in the scope of this research, the linked reactions of NO<sub>x</sub> and VOCs will be discussed.

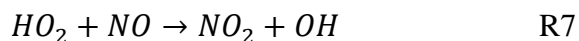
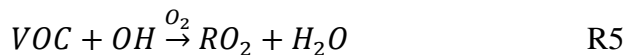
The photolysis of NO<sub>2</sub> in the atmosphere will result in NO and O which, in turn will result in the production of O<sub>x</sub>:



With just reaction 3, NO<sub>2</sub> will be quickly depleted; to restore the concentration of NO<sub>2</sub>, additional reactions with NO must be coupled to the reaction 3. Several reactions are coupled with the NO<sub>2</sub> destruction equation. In the absence of other reagents, NO and O<sub>3</sub> can react to restore NO<sub>2</sub> and O<sub>2</sub> resulting in a null cycle:



In the presence of VOCs, other pathways are preferred resulting in net O<sub>3</sub> production since the O<sub>3</sub> is not destroyed in reaction 4. A multiple-step generic pathway for VOCs:





In this pathway, a VOC reacts with OH in the presence of oxygen to form RO<sub>2</sub> (R indicates a generic carbon structure) and water by transferring a hydrogen atom to the OH. This modified VOC structure then can react with NO to form HO<sub>2</sub> and NO<sub>2</sub>. The HO<sub>2</sub> can then go on to react with a second NO to form another NO<sub>2</sub> molecule and restore the original OH. Overall, this pathway nets out to:



This pathway restores the NO<sub>2</sub> molecules for the O<sub>3</sub> production reaction which means as long as there are both NO<sub>x</sub> (for O<sub>3</sub> production) and VOCs (for restoring the NO<sub>x</sub>) in the troposphere, O<sub>3</sub> production can occur. Since both are required, an atmosphere with only one or the other cannot produce O<sub>3</sub>. An atmosphere with a high mixing ratio in one and limited mixing ratio in the other will be sensitive in changes in the mixing ratio of the limited concentration species. High NO<sub>x</sub> and low VOC makes for a VOC-limited regime and high VOC and low NO<sub>x</sub> makes for a NO<sub>x</sub>-limited regime. Limited mixing ratio of both species make for a regime that is sensitive to changes in both species.

Ozone production can also happen in remote locations due to transport of trace gases. NO<sub>x</sub> has reservoir species such as PAN that have a much longer lifetime in the atmosphere. PAN can be transported by bulk wind from emission sources to far downwind locations and then thermally decompose to reform NO<sub>2</sub>. In this way, remote locations with VOC emissions but low emissions of NO<sub>x</sub> can still experience significant O<sub>3</sub> production due to transport of reservoir species. Since VOCs have a short lifetime in the atmosphere, the inverse is unlikely; transport of VOCs to a remote location to increase O<sub>3</sub> production is unlikely.

## **1.3 State of Research**

### **1.3.1 OMI Retrieval Campaigns**

Retrieval campaigns have been using data from OMI since its launch in 2004 and from its predecessor instruments as well. One such campaign using early OMI data showed that NO<sub>2</sub> columns from the satellite instrument are in agreement with ground-based instruments when it comes to trends, however, OMI underestimates the columns measured by ground instruments by 11 to 36 percent depending on season and land use [Lamsal et al 2008]. Another campaign used OMI data of HCHO columns compared to aircraft measurements to find that OMI can have up to a 17 percent underestimation bias compared to other methods although this might be due to preferential sampling of pollution plumes by other instruments [Boeke et al 2011]. Boecke et al also showed that temporal averaging can help to improve detection limits of retrieved gases although quantification of the effect of this averaging is difficult to determine [Zhu et al 2014]. Zhu et al [2014] used OMI to retrieve HCHO column density in eastern Texas using an oversampling method. In their study, they also found that HCHO column density is dependent on temperature which may indicate a seasonal dependence. Abbot et al [2003] found that HCHO columns retrieved with GOME were consistent with seasonal patterns, current isoprene emission models, and interannual variability of surface temperature. Column densities of HCHO being consistent with the temperature dependence of isoprene emissions is also confirmed in another GOME study [Palmer 2003]. Boersma et al [2007] developed an algorithm to take OMI data and retrieve the column densities of NO<sub>2</sub> in near-real-time in less than three hours. Other algorithms have been developed to retrieve the NO<sub>2</sub> column density using OMI data and taking into account stratospheric contributions, air mass factors (AMF), and other parameters [Bucsela et al 2006]. Statistical analysis and tools have been performed on OMI data for HCHO and other species to improve the evaluation of satellite data [Kim et al 2011]. Since its original launch, algorithms and data products have been in constant improvement and should be capable of retrieving accurate column densities of NO<sub>2</sub>, HCHO, and other trace gases.

### **1.3.2 Formaldehyde-to-NO<sub>2</sub> Ratio**

An important secondary measurement useful in understanding the atmospheric chemistry of regions is the formaldehyde-to-NO<sub>2</sub>-ratio (FNR) [Duncan et al 2010]. Similar research has also been performed with other instruments and models including the GOME satellite instrument [Martin et al 2004a,b]. Because O<sub>3</sub> production is sensitive to either changes in NO<sub>x</sub> or VOC concentration depending on the current concentrations of the two chemical families, a ratio between them can be an indicator of whether the region is in the NO<sub>x</sub>-limited regime or the VOC-limited regime. It can be difficult to compare the total atmospheric content of both chemical families but since OMI can measure NO<sub>2</sub> from the NO<sub>x</sub> family and HCHO from the VOC family, the ratio between them, FNR, can be calculated and used to characterize the ozone production regime. Duncan et al 2010 found that a FNR greater than 2 indicates a NO<sub>x</sub>-limited regime where changes in NO<sub>x</sub> lead to significant changes in O<sub>3</sub> and a FNR lower than 1 indicates a VOC-limited regime where changes in VOC lead to significant changes in O<sub>3</sub>. A FNR between 1 and 2 is limited by both chemical families and so changes in either can lead to significant changes in O<sub>3</sub>. It was determined by Duncan et al that cities tend to have lower FNR values, indicating more sensitivity to VOCs, where rural areas tend to have higher FNR values, indicating more sensitivity to NO<sub>x</sub>.

This research plans to expand on Duncan et al by extending study of FNR to rural areas of the Great Lakes region not covered in their study. The Duncan et al study lacked data for this region and the goal is to determine whether OMI is sensitive to retrieving low levels of NO<sub>2</sub> and HCHO in order to calculate FNR in these regions.

### **1.4 Objectives and Hypotheses**

This research will aim to answer the following questions using OMI. Geographic focus will be on the western Great Lakes region:

- Is the OMI instrument sensitive to changes in concentration of gases near to the ground? Do the OMI column densities of NO<sub>2</sub> and ground-based concentrations of NO<sub>2</sub> in rural display similar temporal trends?
- Can a gradient of NO<sub>2</sub> and HCHO and FNR from urban areas to rural areas be retrieved using OMI? Are these gradients statistically significant given the errors inherent to the instrument and technique?
- Can OMI detect the O<sub>3</sub> production regime a region is in and where the regime changes from one to another?
- Is there a seasonal dependency to FNR values? Are they significantly higher in one season or another?

Based on previous studies, my hypothesis for these questions is that OMI will be usable in rural areas for research purposes. The instrument should be sensitive to changes in gas concentration at the surface, changing with day-of-week and month-of-year in the same manner as ground instruments. Gradients from urban-to-rural should be retrievable using OMI for NO<sub>2</sub>. It is known that the concentrations of NO<sub>2</sub> are higher in urban areas than rural areas so the question is not if there is a gradient but whether or not OMI can retrieve a significant gradient taking into account the inherent error and the detection limits.

HCHO, in comparison, may not have a retrievable gradient. However this may be because there is no gradient or significant difference between urban columns and rural columns. HCHO will be somewhat similar between the city and rural areas because there are significant sources in both.

Because NO<sub>2</sub> will have a significant gradient and HCHO will not have a significant gradient, it can be concluded that there will be a significant gradient in FNR with the FNR low in urban areas and high in rural areas. Due to propagation of errors and the high inherent errors present in the current OMI instrumental technique, the exact borders between regimes may be difficult to determine. In order to definitively place a region in one regime or the other, the FNR value must be much higher than 2 or much lower than 1. Between these two adjusted values, the regime and chemistry is not well

known using OMI data. This research should be able to locate some regions clearly in the VOC-limited regime and some regions clearly in the  $\text{NO}_x$ -limited regime. FNR is hypothesized to be higher in summer than in winter because of expected higher  $\text{NO}_2$  concentrations in winter and higher HCHO concentrations in summer.

## **1.5 Outline of Thesis**

Methodology and research design is discussed in Chapter 2, including how the data was obtained, processed, and analyzed and the error analysis. Results and data are presented in Chapter 3, including weekly and monthly analyses of  $\text{NO}_2$ , HCHO, and FNR in urban and rural regions. A discussion of the research is given in Chapter 4, including the implications and successes of the research. Conclusions are given in Chapter 5, including future work and possible improvements to the research.

## **2. Methodology**

### **2.1 Data Collection**

OMI is onboard the AURA satellite orbiting the Earth 14 times a day in a sun-synchronous polar orbit at an altitude of 705 km. Like its predecessors the European Global Ozone Monitoring Experiment (GOME) instrument, Scanning Imaging Absorption Spectrometer for Atmospheric Chartography (SCIAMACHY) instrument, and Total Ozone Mapping Spectrometer (TOMS) instrument, OMI measures light in the UV/VIS spectrum with a high spatial resolution for a satellite instrument. OMI is capable of covering the entire globe once daily at approximately the same local time around the globe; the local time of crossing the equator is between 13:40 and 13:50. [Levelt et al 2006]

Due to the nature of satellite remote sensing, the eventual data product for gases is a column density from the satellite, from the top of atmosphere, to the ground. To determine the column density of gases, the Differential Optical Absorption Spectroscopy (DOAS) algorithm is used. DOAS is a remote sensing technique for measuring the

concentrations of gases in a target air mass [Platt and Stutz 2008]. What separates it from other techniques is the differentiating of narrow absorption features of the target species from the broad absorption features occurring in the atmosphere at large. Radiation propagating through the atmosphere is absorbed by gases in the atmosphere as well as scattered from both gases and aerosols.

The DOAS technique, like many other optical remote sensing techniques uses the Beer-Lambert Law. Differentiating the broad and narrow features will divide the exponent in the Beer-Lambert Law into an exponent for the broad features and an exponent for the narrow features [Platt and Stutz 2008].

$$I(\lambda) = I_0(\lambda)e^{(-\tau_b)}e^{(-\tau_n)} \quad \text{R9}$$

$I$  is the transmitted light that reaches the detector after absorption and scattering and  $I_0$  is the incident light from the light source. The first exponent term is simplified here as  $\tau_b$ . However, this is the sum of the optical depths (or the sum of the products of path length and extinction coefficients) of all of the broad spectrum features: background gas species, background aerosol species, and other broad spectrum effects. The second exponent term contains  $\tau_n$  which is likewise the sum of optical depths for all of the narrow spectrum features: the trace gases of interest. To simplify the equation above, we can rewrite the broad spectrum term and the incident intensity as a single term. [Platt and Stutz 2008]

$$I'_0 = I_0(\lambda)e^{(-\tau_b)} \quad \text{R10}$$

$$I(\lambda) = I'_0(\lambda)e^{(-\tau_n)} \quad \text{R11}$$

As the exponential term contains the optical depths of the target species, this is dependent on path length ( $L$ ), absorption cross section ( $\sigma$ ), and number density of each species ( $N$ ):

$$I(\lambda) = I'_0(\lambda)e^{(-L*\sigma*N)} \quad \text{R12}$$

DOAS instruments measure the intensity of incoming light ( $I$ ) over a wavelength band, which is dependent on the optical system used. A polynomial function is fitted to the spectra to remove the broad features owing to scattering. The narrow features, due to absorption of gases in the atmosphere, remain. Cross sections for each target gas as well as a Ring function and polynomial are then fitted to the narrow features in the spectra to retrieve the number density of each gas [Platt and Stutz 2008]. A Fraunhofer reference spectrum is used to eliminate the Fraunhofer lines from the measured spectra. For a passive DOAS system, like the one used in this study, the path length is unknown so a slant column density is determined (in units of molecules-cm<sup>2</sup>), which is the product of the number density and the path length ( $SCD=L*N$ ).

OMI can retrieve NO<sub>2</sub> column densities because NO<sub>2</sub> has an absorption cross-section in the spectral range of the instrument. Since NO<sub>x</sub> is a chemical family with rapid cycling between NO and NO<sub>2</sub>, retrieval of NO<sub>2</sub> can be used to obtain information about total NO<sub>x</sub> column density in the atmosphere. Similarly, OMI can retrieve HCHO column densities but not all VOCs. The HCHO column density can be used as an indicator of total VOC content however for atmospheric chemistry analysis.

OMI measures light in two channels: the UV channel and the VIS channel. The VIS channel measures between 365 and 500 nm and is used to retrieve NO<sub>2</sub> as well as some aerosols, cloud cover, and other data products. The UV channel is subdivided into UV-1 and UV-2 subchannels. UV-2 measures between 310 and 365 nm and is used to retrieve HCHO as well as O<sub>3</sub> column, BrO, SO<sub>2</sub>, some aerosols, cloud cover, and other data products. UV-1 measures from 270-310 nm and measures several data products. The instrument is nadir pointing with a field of view of 114° for a swath width of 2600 km which covers the globe in 14 orbits a day. This swath is divided into pixels of dimensions 13 km x 24 km. [Levelt et al 2006]

Data from OMI was downloaded using the Mirador data tool on the NASA website (<http://mirador.gsfc.nasa.gov/>) for the time period of January 1, 2011 through December 31, 2014. The OMI data products used were the Level-3 NO<sub>2</sub> Cloud-Screened Total and Tropospheric Column NO<sub>2</sub> data (OMNO2d) and the OMI Global

Level-2G Formaldehyde Data Product data (OMHCHOG). The Level-3 NO<sub>2</sub> data is the most up to date NO<sub>2</sub> data from OMI using a revised algorithm and taking into account cloud cover data from OMI to provide preliminary cloud-screening. The Level-2 HCHO data is the most up to date for HCHO from OMI; Level-3 HCHO data is not available. The Level-2 HCHO data does not include several forms of screening present in the Level-3 data which means cloud screening was performed on the data set prior to analysis.

Global data for each day were downloaded and processed using IDL programs written at Michigan Technological University. These programs corrected for cloud cover in the level-2 HCHO data and filtered for detection limit thresholds. Each pixel represents a 0.25 by 0.25 degree section of the surface.

Detection limits used for analysis were obtained from the literature. For HCHO, detection limit estimates are  $4.0 \times 10^{15}$  molecules/cm<sup>2</sup> [Chance et al 2000] and  $3.0 \times 10^{15}$  molecules/cm<sup>2</sup> [Gonzalez Abad et al 2014]. Detection limit estimates of NO<sub>2</sub> found are between  $0.1$  and  $0.2 \times 10^{15}$  molecules/cm<sup>2</sup> [Boersma et al 2007]. The higher detection limits of  $4.0 \times 10^{15}$  molecules/cm<sup>2</sup> for HCHO and  $0.2 \times 10^{15}$  molecules/cm<sup>2</sup> for NO<sub>2</sub> were used in this research to be conservative. These detection limits were used to filter the data prior to analysis. Out of the 1,831,680 total data point pixels in this research, only 39,103 HCHO pixels were dropped due to detection limit – 2.135 percent of all the pixels – and only 14936 NO<sub>2</sub> pixels were dropped – 0.815 percent of all the pixels.

The daily data was then processed to calculate FNR from the NO<sub>2</sub> and HCHO column densities over the Great Lakes region, defined by map coordinates of 48° to 40° latitude and -90° to -80° longitude. After this step, daily data points for both trace gas species and FNR for each pixel in the Great Lakes region were saved and can then be analyzed.

Because of the nature of satellite retrievals, there may not always be a value for a specific pixel on a specific day. The pixel may have been cloud screened or the trace gas may not be above the detection limit or there may be some other issue with obtaining column density for that pixel on that day. Because of this, there may be insufficient data to calculate the FNR for a specific pixel on a specific day. This problem requires analysis to be performed and averaged over years of data to improve the coverage of an area.



## 2.2 Error Analysis

Error for the average column densities are calculated using the values mentioned in Duncan et al 2010. The authors estimated an error for NO<sub>2</sub> column density to be 10-40 percent and an estimated error for HCHO column density of 25-31 percent. Sources of error in NO<sub>2</sub> column densities using OMI include errors in surface albedo values, errors in cloud fraction and cloud pressure retrievals, and errors in profile shape which create errors in the calculated AMF [Boersma et al 2007]. There are also fitting errors in the DOAS technique derived as well that contribute to overall error. Errors in HCHO column density arise from errors in calculated AMF from surface albedo, errors in profile shape, errors in aerosol effects, and errors in cloud effects [Millet et al 2006]. Again, there are fitting errors as well from the DOAS technique that contribute to total error in HCHO. In areas with low values of HCHO and over oceans the error in column density comes mainly from the fitting errors but over continental areas and areas with higher values of HCHO, the errors from AMF are more relevant [Hewson et al 2015]. The Great Lakes region to be studied is a continental area but according to findings from previous studies such as Duncan et al 2010, the region is at neither a high nor a low concentration of HCHO. It is difficult to say whether the AMF errors or the fitting errors are dominant in the region.

If most of the error is due to error in AMF which is a systematic error, the error is difficult to reduce in post-retrieval analysis and must be reduced during the retrieval and processing steps of using OMI which is outside the scope of this work.

As a result of the estimates for error in NO<sub>2</sub> and HCHO, the double-ended error bars for the results will be set at 40 percent for NO<sub>2</sub> and 31 percent for HCHO which will give a worst-case scenario approach to whether or not OMI can be used for this research. Assuming the errors in HCHO and NO<sub>2</sub> are not correlated, by propagation of errors, the error in FNR will be 51 percent.

Alternate error analysis can be performed to calculate the standard deviation from averaging the pixels in the region and over time. This standard deviation should represent the errors resulting in the statistics of the technique performed. Together with the instrumental error, the total error can be better understood.

Errors may be present in OMI data products that may cause systematic disagreement with other instruments or the true column density of the atmosphere. However, since the nature of this research is to compare OMI data to OMI data, these bias errors will disappear if they are assumed to be systematic to the instrument. Lamsal et al [2008] and Boeke et al [2011] estimate that the OMI instrument underestimates the column density in HCHO and NO<sub>2</sub> by a fixed percent; the OMI data will be low by the same fixed percent across the analysis. Because of this, the systematic errors of the instrument can be ignored when running analysis of OMI data across seasons and across the week. Because the systematic errors may not be the same across target species, they cannot be ignored or canceled when analyzing multiple species such as with FNR.

### **2.3 Data Processing**

Once processed, the data gives the daily columns of NO<sub>2</sub> and HCHO, tropospheric for the NO<sub>2</sub> and full column for the HCHO, and the FNR for each 0.25° by 0.25° pixel in the Great Lakes region. The NO<sub>2</sub> column has the stratospheric portion removed and the full column of HCHO is representative of the tropospheric column as there should be no HCHO in the stratosphere. This data was used to produce map plots of the Great Lakes region for all three parameters for each month of 2011 to 2014; each pixel is the monthly average for that pixel, not including the days when there is no data. This serves to visualize the column densities and FNR for the whole region for each month and is a rough view of whether or not the data will be sufficient to analyze further.

To determine the sensitivity of OMI to changes at the surface, the processed NO<sub>2</sub> data was compared to ground-based data from EPA sites. Data from both were binned by day-of-week and also by month and then averaged. Although the two data sets provide measurements at different scales – vertical column density from OMI (in molecules per cm<sup>2</sup>) and number density from in situ ground-based instruments (in parts per billion

(ppb)) – the relative changes can be compared between the two. If OMI detects the same weekly and annual trends as the ground instruments, it can be considered to be sensitive to changes in NO<sub>2</sub> near the ground. Four sites were analyzed to determine the sensitivity of OMI to changes in concentrations near to the ground: Chicago, Milwaukee, Manitowoc, and the Potawatomi Reservation. These four sites correspond to the region for research later in this project and also correspond to a land use change from urban to rural. Permanent ground sensors are not present in northern Wisconsin or the Upper Peninsula of Michigan to represent a rural wilderness Great Lakes region. Each of the three sites has a ground-based NO<sub>2</sub> sensor managed by the EPA. OMI data from the pixels within a 0.5 x 0.5 degree box around the ground-based sensor were analyzed for NO<sub>2</sub> column density.

Processed data was used to answer the research questions in two linear regions: the line between Chicago and the Keweenaw Peninsula and the line between Detroit and the Mackinac Bridge. The purpose of this is to look at two expected gradients of urban to rural. Both Chicago and Detroit represent urban areas and serve as one extreme of the expected gradients. The Keweenaw Peninsula and the Mackinac Bridge represent rural areas to serve as the other extreme. Between Chicago and the Keweenaw Peninsula and Detroit and the Mackinac Bridge should be a transition from urban to rural with smaller urban areas and varying rural land use categories. FNR values were also compared across seasons to determine if the temperature dependence of HCHO and any seasonal dependence in HCHO and NO<sub>2</sub> creates seasonal trends in FNR.

### **3. Results**

#### **3.1 Comparison to Ground-Based Instruments**

By comparing ground-based instruments to OMI, the ability of OMI to retrieve column densities that are representative of ground based emissions of NO<sub>2</sub> can be assessed. For large concentrations of NO<sub>2</sub> in urban areas, OMI has been shown to be capable of retrieving changes in NO<sub>2</sub> concentration but this research will investigate the ability to retrieve changes in rural areas as well.

The first of the four sites to consider is in Chicago at coordinates (41.86, -87.75). The ground based NO<sub>2</sub> mixing ratios are at their highest during February and lowest during July with the lowest values being 57.7 percent of the highest value. In general, the concentrations are higher in the winter than the summer (Figure 1a, blue line). The OMI column densities follow the same general curve (Figure 1a, red line) rising in the winter and falling in the summer. The highest density is instead in January and the lowest density is in July with the lowest being 34.8 percent of the highest. From the ground instrument, the NO<sub>2</sub> mixing ratios are slightly higher on Fridays than the rest of the week and slightly lower on Sundays than the rest of the week (Figure 1b, blue line). The OMI column densities follow this same trend with higher values on Fridays and lower values on Sundays (Figure 1b, red line).

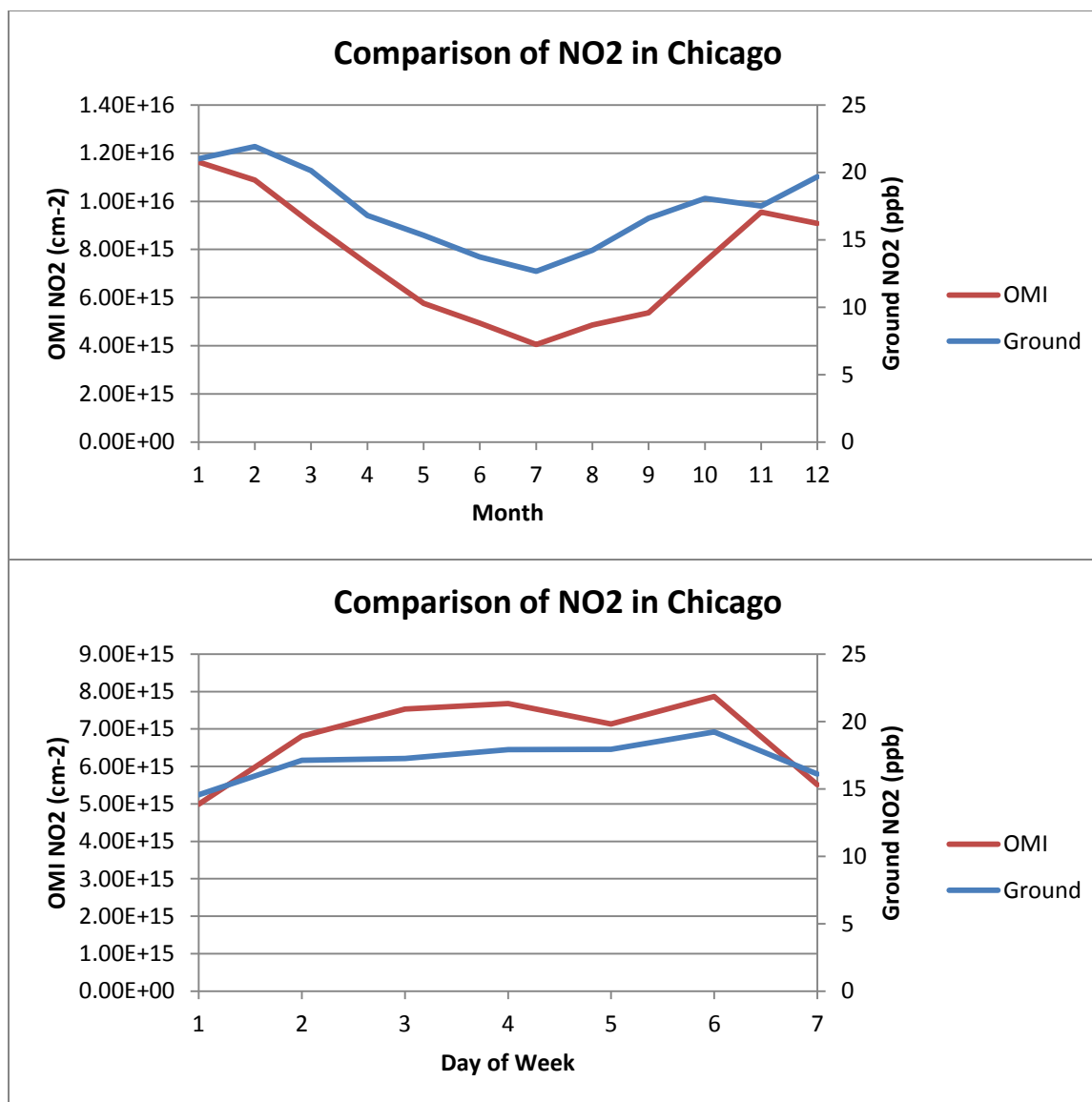


Figure 1: OMI column densities and ground instrument mixing ratios of NO<sub>2</sub> by (1a, top) month and (1b, bottom) day of week in Chicago.

At the second site in Milwaukee at (43.06, -87.91), the ground-based instrument retrieves higher NO<sub>2</sub> concentrations in winter and lower concentrations in summer, reaching a maximum in February and a minimum in July (Figure 2a, blue line). The lowest mixing ratio is 54.9 percent of the highest mixing ratio. OMI retrieved higher column densities in winter and lower in summer as well but with the maximum in November and the minimum in July (Figure 2a, red line). The lowest column density is

22.0 percent of the highest. For NO<sub>2</sub> retrievals from both ground instrument and OMI the concentrations are largely constant across the week with the OMI column densities peaking on Tuesdays and the ground instrument's concentration peaking on Fridays and both at a minimum on Sundays (Figure 2b).

The third site is in Manitowoc at (44.14, -87.62). There is no NO<sub>2</sub> data for October through April from the ground instrument but for the five summer months there is data for, the peak is in June (Figure 3a, blue line). The OMI data has column densities for the whole year with the highest NO<sub>2</sub> in January and the lowest NO<sub>2</sub> in August (Figure 3a, red line). Data analysis for mixing ratios by day of week reveals similar weekly trends for both OMI and ground instruments, staying constant through the week and dropping slightly on Sundays (Figure 3b).

The fourth site is on the Potawatomi Reservation in northern Wisconsin at (45.56, -88.81). The NO<sub>2</sub> mixing ratios are higher in winter than summer but there is a local maximum in May and June (Figure 4a, blue line). These higher mixing ratios in summer are not an artifact of the averaging over year; the years 2011, 2012, and 2013 all have elevated mixing ratios during those months. The data for 2014 appears to be missing for most of the year. The lowest mixing ratio in April is 24.8 percent of the highest mixing ratio in January. NO<sub>2</sub> retrievals from OMI also show the highest column densities in winter and lowest in summer but without the local maximum present in the ground instrument (Figure 4a, red line). The lowest mixing ratio in July is 30.3 percent of the highest mixing ratio in January. Both ground instrument and OMI show constant NO<sub>2</sub> across the days of the week (Figure 4b).

Overall, the results indicate that OMI is in agreement with ground based instruments and is able to detect changes in NO<sub>2</sub> concentrations near to the ground. OMI is able to be used to measure NO<sub>2</sub> near to the ground and NO<sub>2</sub> column density should be representative of the ground concentrations.

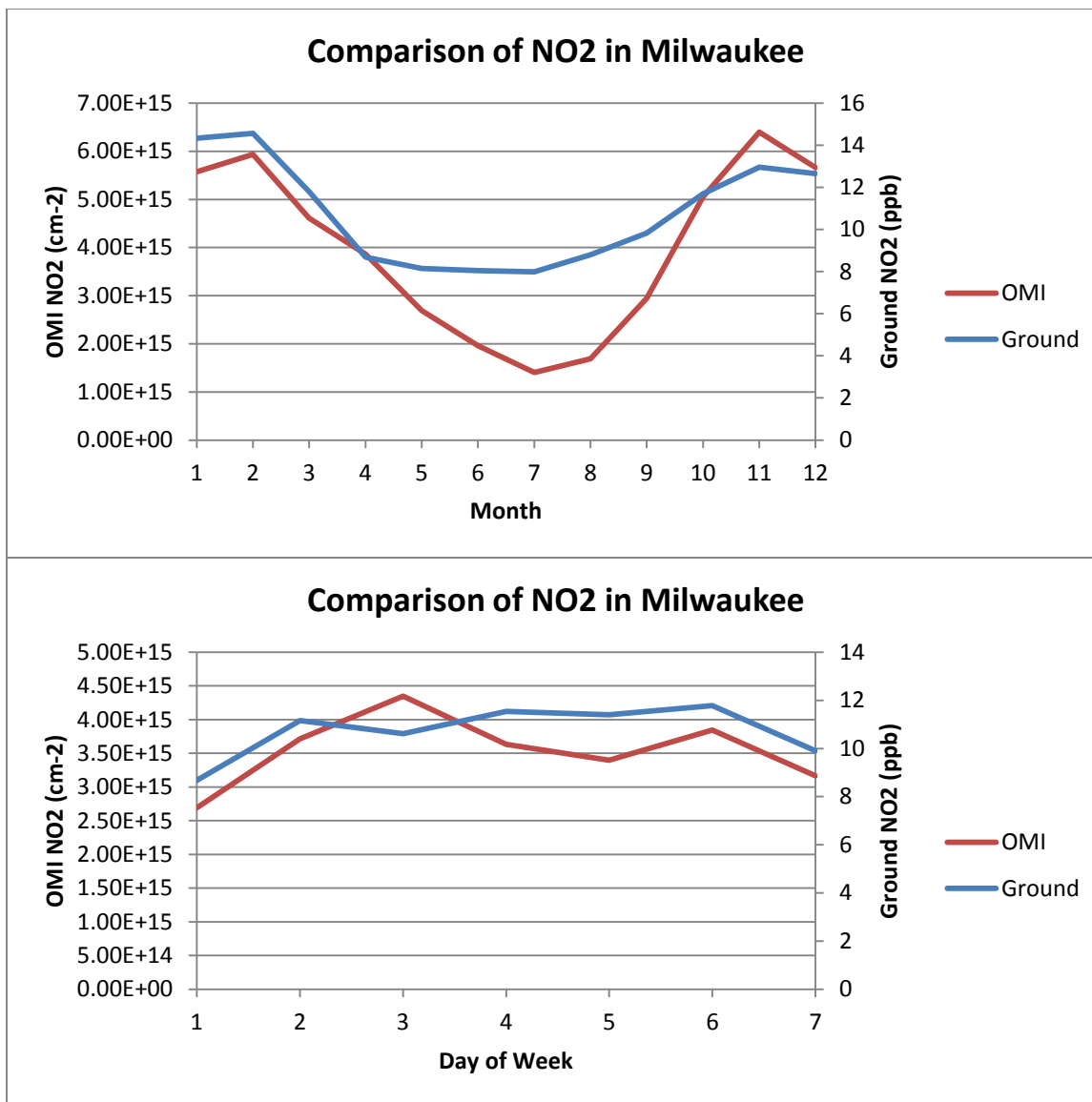


Figure 2: OMI column densities and ground instrument mixing ratios of NO<sub>2</sub> by (3a, top) month and (3b, bottom) day of week in Milwaukee.

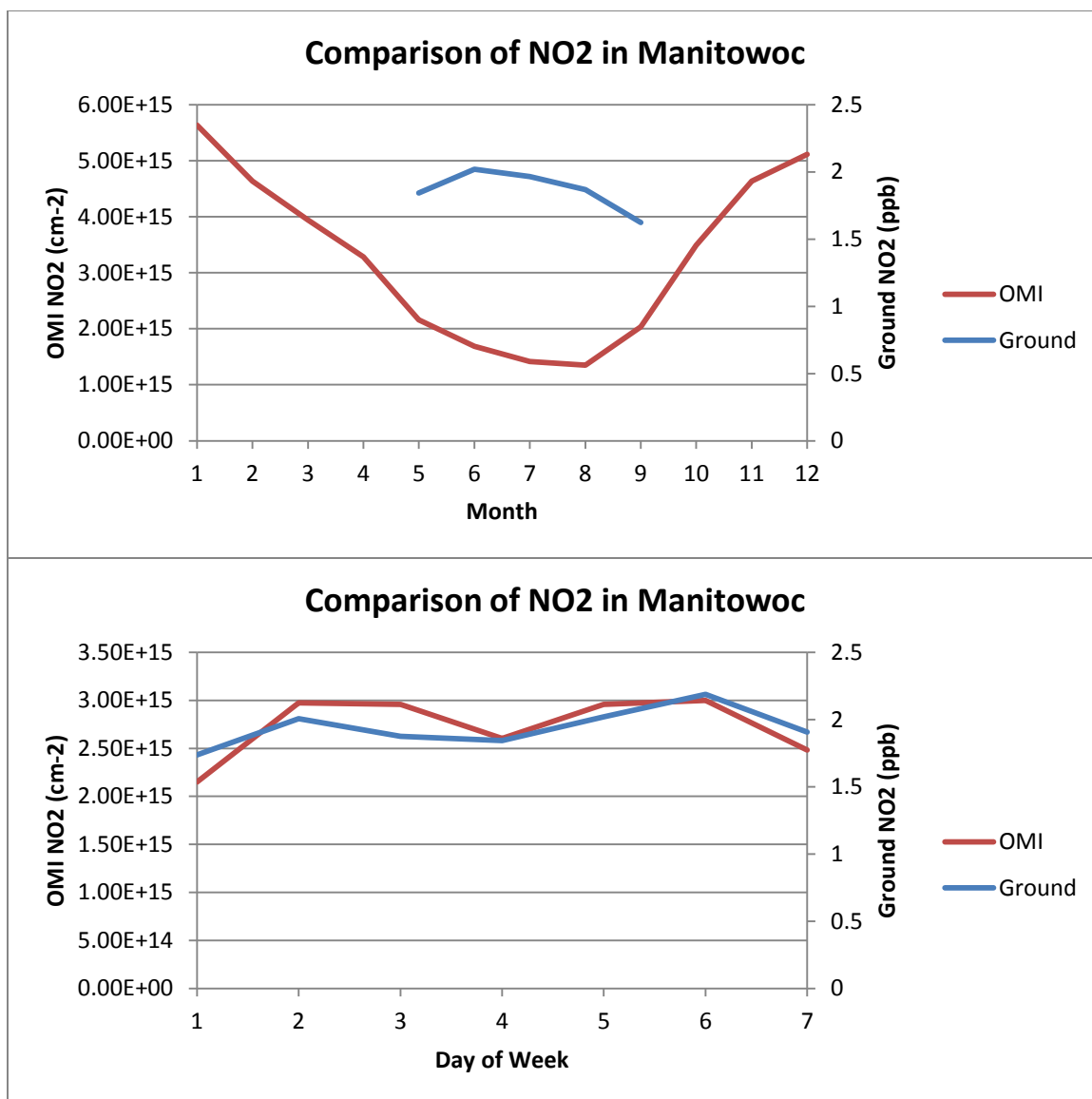


Figure 3: OMI column densities and ground instrument mixing ratios of NO<sub>2</sub> by (4a, top) month and (4b, bottom) day of week in Manitowoc.



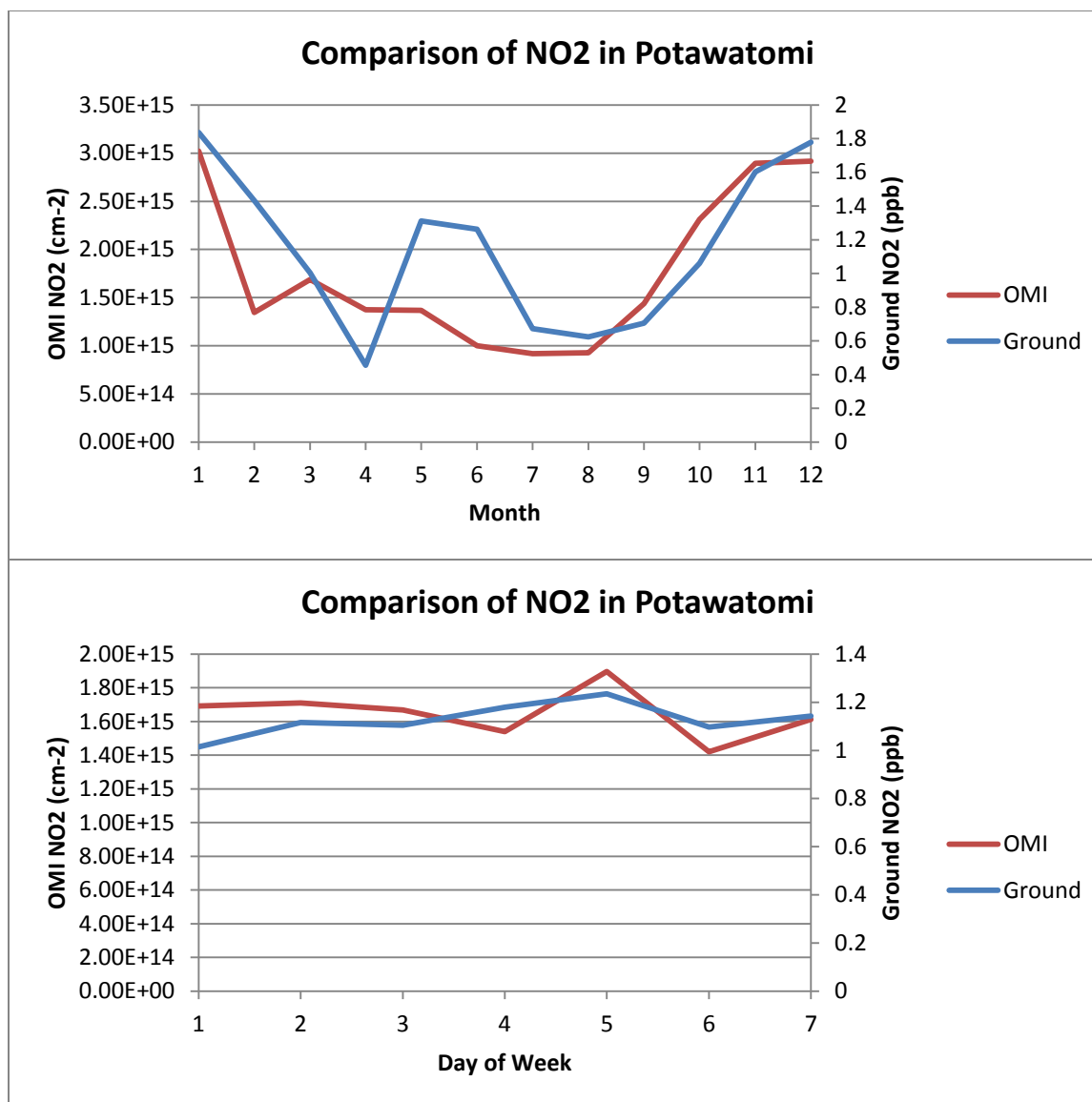


Figure 4: OMI column densities and ground instrument mixing ratios of NO<sub>2</sub> by (5a, top) month and (5b, bottom) day of week in Potawatomi.

### 3.2 Gradient from Chicago to the Keweenaw Peninsula

Using the OMI data, two gradients were analyzed for three parameters: NO<sub>2</sub> column density, HCHO column density, and FNR. In doing so, it can be determined whether or not OMI is capable of resolving a significant gradient between urban areas and rural areas for the three parameters. Using urban areas such as Chicago and Detroit and rural areas such as the UP of Michigan and the northern point of the LP of Michigan should make

for the best chance of getting a strong gradient for analysis. Analysis will be divided into four seasons as there is great variability in the annual cycles of the species as shown in the previous section.

The first of the two gradients to be analyzed is between the Chicago metropolitan area (41.9°N, 87.7°W) and the base of the Keweenaw Peninsula in the Upper Peninsula (UP) of Michigan (47.0°N, 88.7°W). The line between these two regions passes through the heavy urban land use of Chicago itself, the dense suburban sprawl of Chicago suburbs, smaller cities of Milwaukee and Green Bay, large highways through Wisconsin, rural northern Wisconsin towns, and the forested wilderness of the UP. This line should cover a land use gradient from urban to rural along its length. Along the gradient, column densities of NO<sub>2</sub> and HCHO were retrieved every 0.25 degrees of latitude. From these column densities, FNR was calculated for the same latitude intervals. Error bars are included using the error estimates presented in the previous chapter: 40 percent for NO<sub>2</sub> column, 31 percent for HCHO column, and 51 percent FNR from propagation of errors.

As there may be differences between seasons for the column densities and the FNR, the analysis was performed by season. Values for each day's pixel containing the gradient line were compiled across all four years 2011 to 2014 and averaged together to give a single value for column density for each season. For the purposes of this research, winter is considered to be January, February, and December; spring is considered to be March, April, and May; Summer is considered to be June, July, and August; and Fall is considered to be September, October, and November. Thus, the analysis for winter has all of the days of January, February, and December from 2011, 2012, 2013, and 2014 averaged together at each pixel along the gradient line.

Satellite data for winter can be found in Figure 5 below. Figure 5a shows that the gradient from high NO<sub>2</sub> column densities (red color) to low column densities (blue color) appears to correspond with the line between Chicago and the Keweenaw with the high density in urban Chicago and the low densities in rural Wisconsin and the UP. There does not seem to be any clear gradient for the HCHO data (Figure 5b) along the line with some pixels being higher densities (lighter blue) and some pixels being lower densities (darker blue).

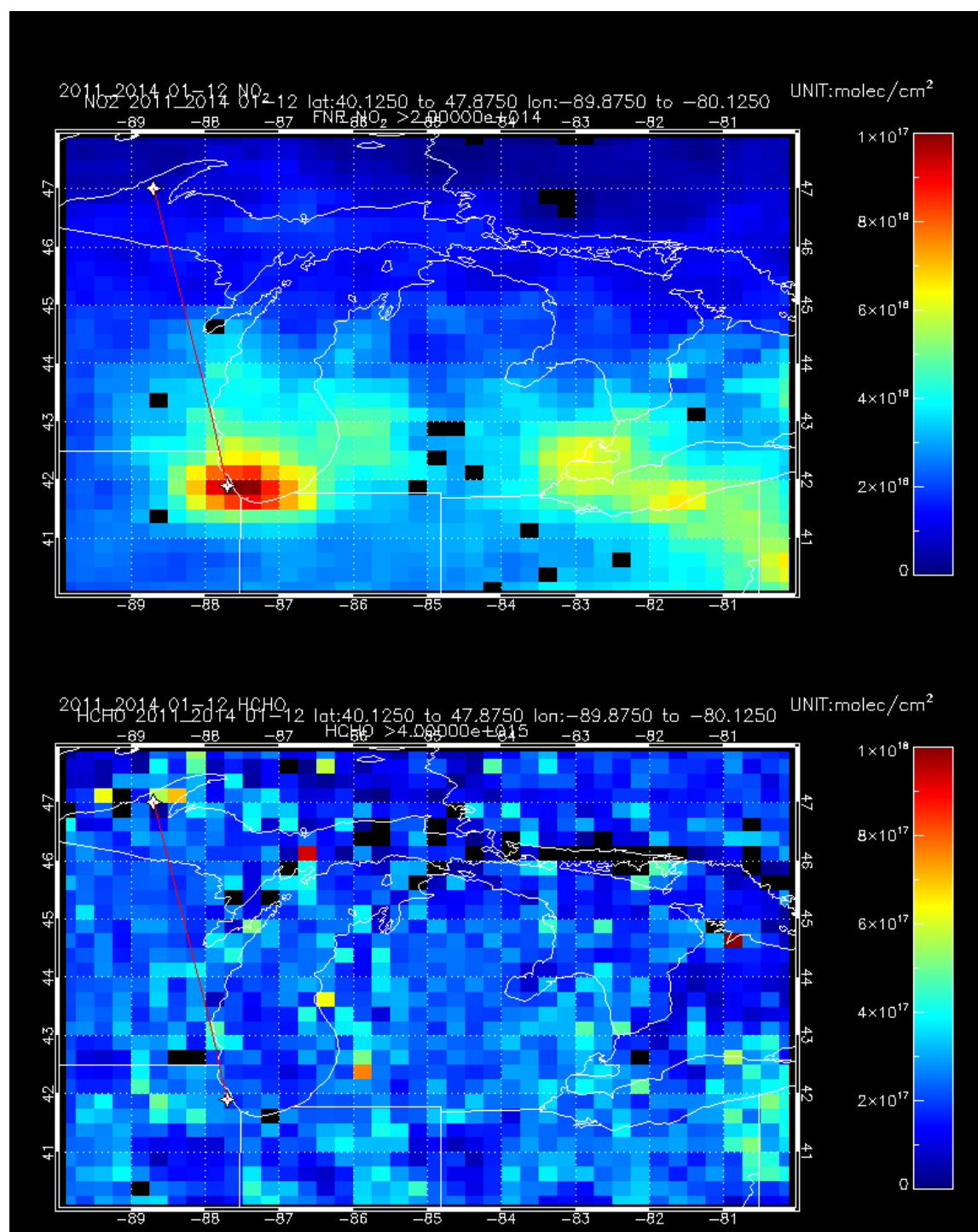


Figure 5: Column densities of (5a, top)  $\text{NO}_2$  and (5b, bottom)  $\text{HCHO}$  from OMI data during winter.

Analysis of the winter data can be found in Figure 6. From Figure 6a, it can be seen that there is a gradient from the lower latitudes to higher latitudes. Taking into account the error bars, the points corresponding to Chicago are statistically higher than the points corresponding to rural Wisconsin and the UP of Michigan. The lowest column density is  $2.33 \times 10^{15} \text{ cm}^{-2}$  at  $47^\circ\text{N}$  which compared to the highest column density of  $1.18 \times 10^{16} \text{ cm}^{-2}$  at  $41.9^\circ\text{N}$  is only 19.7 percent of the highest density. This difference is outside the error bars for both points.

The plot of winter HCHO shows no significant gradient or difference across the line. There are points that are higher or lower than others but due to the error bars, there is no significant difference to conclude there is a HCHO gradient. There are a few selected points that are higher or lower than others by a percentage greater than the sum of the error bars.

The plot for winter FNR shows a weak gradient from urban to rural with urban areas possessing lower FNR and rural areas possessing higher FNR. Several points further north in the gradient line are significantly higher than the first few points in the urban Chicago area. The lowest FNR is 0.93 at  $41.9^\circ\text{N}$  and the highest FNR is 5.20 at  $46.5^\circ\text{N}$ ; the lowest FNR is 17.9 percent of the highest FNR and the difference is greater than the sum of the error bars. Most of the data points have a FNR above 2 which means these regions have  $\text{NO}_2$ -limited  $\text{O}_3$  production. The first few points have a FNR between 1 and 2 with taking into account error which means these regions have  $\text{O}_3$  production sensitive to changes in both species.

Satellite data for spring is shown in Figure 7 below. As with the winter data, the gradient from high  $\text{NO}_2$  column densities to low column densities appears to correspond with the line between Chicago and the Keweenaw with the high density in urban Chicago and the low densities in rural Wisconsin and the UP. Again, there does not seem to be any clear gradient for the HCHO data along the line with some pixels corresponding to both high and low column densities.

Analysis of the spring data can be found in Figure 8. From Figure 8a, it can be seen that there is a strong gradient in  $\text{NO}_2$  from the lower latitudes to higher latitudes. Taking into account the error bars, the points corresponding to Chicago are statistically higher

than most of the points corresponding to north half of the line which is where the land use changes from cities to small towns. The lowest column density is  $1.37 \times 10^{15} \text{ cm}^{-2}$  at  $47^\circ\text{N}$  which compared to the highest column density of  $7.32 \times 10^{15} \text{ cm}^{-2}$  at  $41.9^\circ\text{N}$  is only 18.7 percent of the highest density. This difference is outside the error bars for both points.

The plot of spring HCHO, just as with the winter HCHO, shows no significant gradient or difference across the line. Unlike the winter data, the spring shows that HCHO is constant along the line with minor changes in the mean column density within the error bars.

The plot for spring FNR shows a weak gradient from urban to rural with urban areas possessing lower FNR and rural areas possessing higher FNR. As with the winter data, several points further north in the gradient line are significantly higher than the first few points in the urban Chicago area. The lowest FNR is 1.65 at  $41.9^\circ\text{N}$  and the highest FNR is 10.7 at  $46.25^\circ\text{N}$ ; the lowest FNR is 15.4 percent of the highest FNR and the difference is greater than the sum of the error bars. Almost all of the data points have a FNR above 2 which means these regions are likely to have  $\text{NO}_2$ -limited  $\text{O}_3$  production. The southernmost point in urban Chicago has a FNR between 1 and 2 which suggests these regions have  $\text{O}_3$  production sensitive to changes in both species. With error potentially pushing it above 2 or below 1, the regime could be  $\text{NO}_x$ -limited or VOC-limited.

Satellite data for summer can be found in Figure 9 below. As with winter and spring, the gradient from high  $\text{NO}_2$  column densities to low column densities appears to correspond with the line between Chicago and the Keweenaw with the high density in urban Chicago and the low densities in rural Wisconsin and the UP. There does not seem to be any clear gradient for the HCHO data along the line with some pixels being higher densities and some pixels being lower densities.

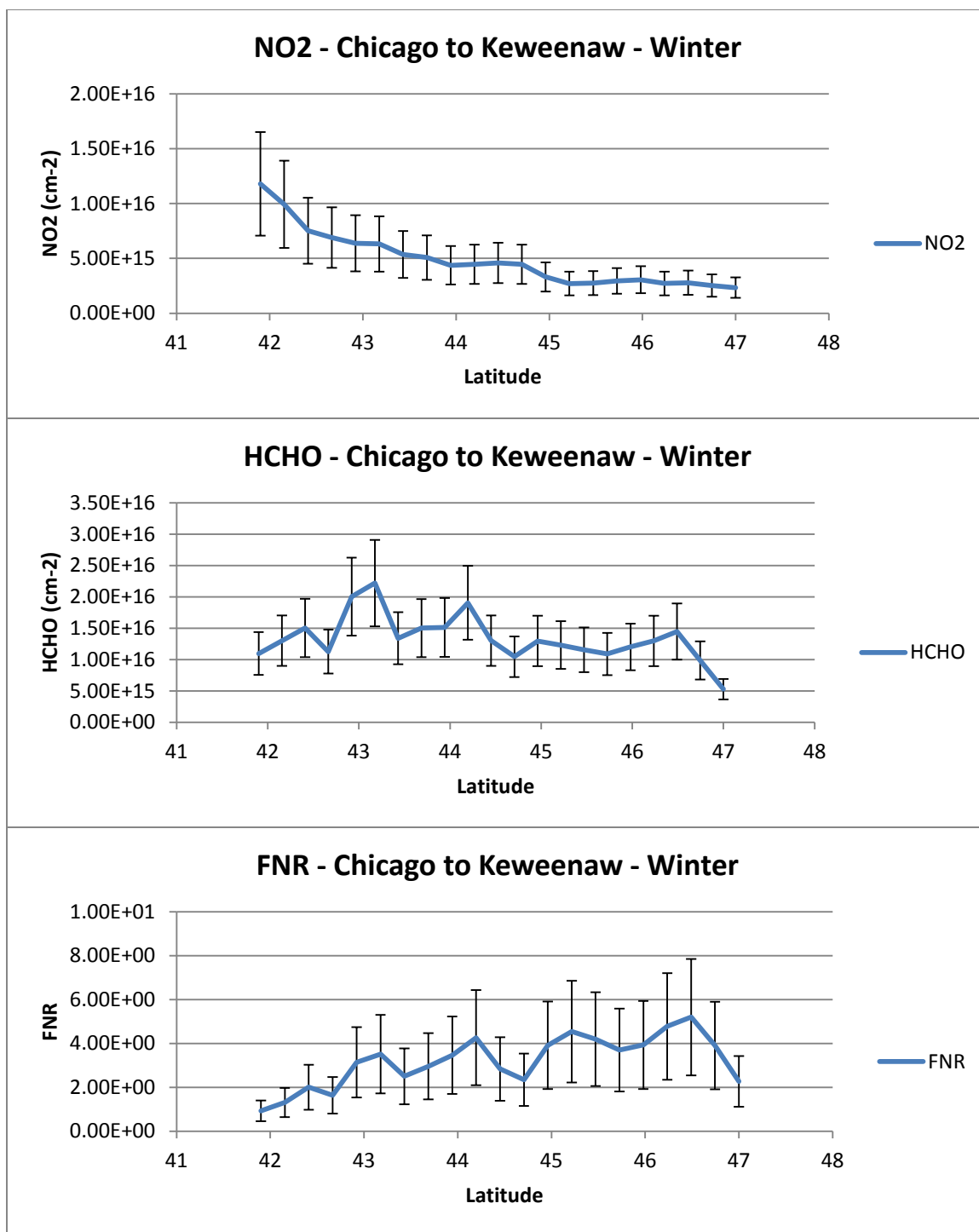


Figure 6: Column densities of (6a, top) NO<sub>2</sub> (6b, middle) HCHO, (6c, bottom) FNR during winter.

Analysis of the summer data can be found in Figure 10. From Figure 10a, it can be seen that there is a strong gradient from the lower latitudes to higher latitudes. Taking

into account the error bars, the points corresponding to Chicago are statistically higher than most of the points corresponding to north half of the line which is where the land use changes from cities to small towns; this is similar to the results for the spring data. The lowest column density is  $9.27 \times 10^{14} \text{ cm}^{-2}$  at  $46.75^\circ\text{N}$  which compared to the highest column density of  $4.68 \times 10^{15} \text{ cm}^{-2}$  at  $41.9^\circ\text{N}$  is only 19.8 percent of the highest density. This difference again is well outside the error bars for both points.

The plot of summer HCHO is much the same as the spring HCHO data and shows no significant gradient or difference across the line. Also like the spring data, the summer data shows that HCHO is constant along the line with minor changes in the mean column density that are very much within the error bars.

The plot for summer FNR shows a weak gradient from urban to rural with urban areas possessing lower FNR and rural areas possessing higher FNR. Like with the winter and spring data, several points further north in the gradient line are significantly higher than the first few points in the urban Chicago area. The lowest FNR is 3.87 at  $41.9^\circ\text{N}$  and the highest FNR is 22.0 at  $46^\circ\text{N}$ ; the lowest FNR is 17.6 percent of the highest FNR and the difference is greater than the sum of the error bars. All of the data points have a FNR above 2 which suggests the whole region has  $\text{NO}_2$ -limited  $\text{O}_3$  production.

Satellite data for fall can be found in Figure 11 below. As with the other seasons, the gradient from high  $\text{NO}_2$  column densities to low column densities appears to correspond with the line between Chicago and the Keweenaw with the high density in urban Chicago and the low densities in rural Wisconsin and the UP. There does not seem to be any clear gradient for the HCHO data along the line with some pixels being higher densities and some pixels being lower densities.

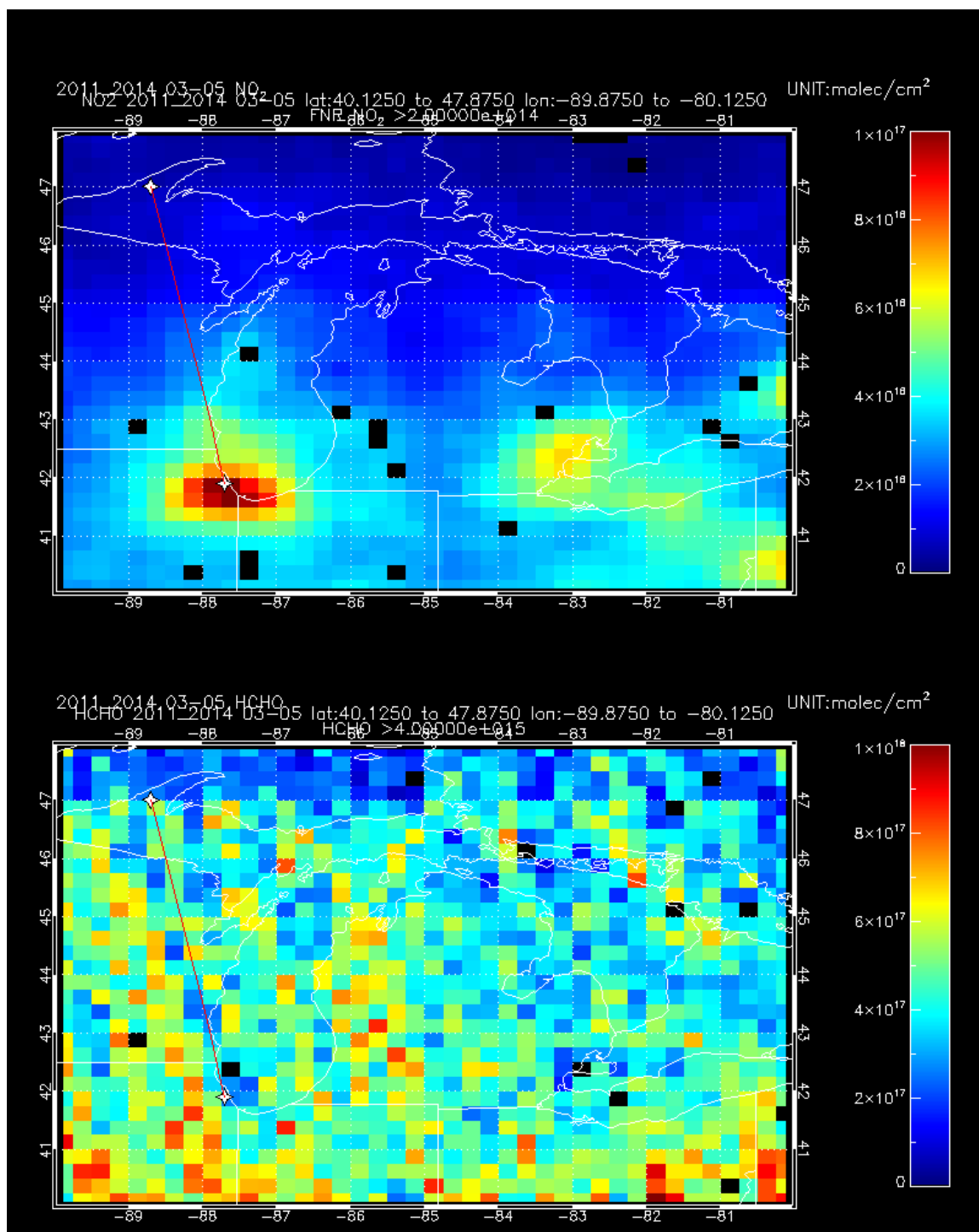


Figure 7: Column densities of (7a, top)  $\text{NO}_2$  and (7b, bottom)  $\text{HCHO}$  from OMI data during spring.



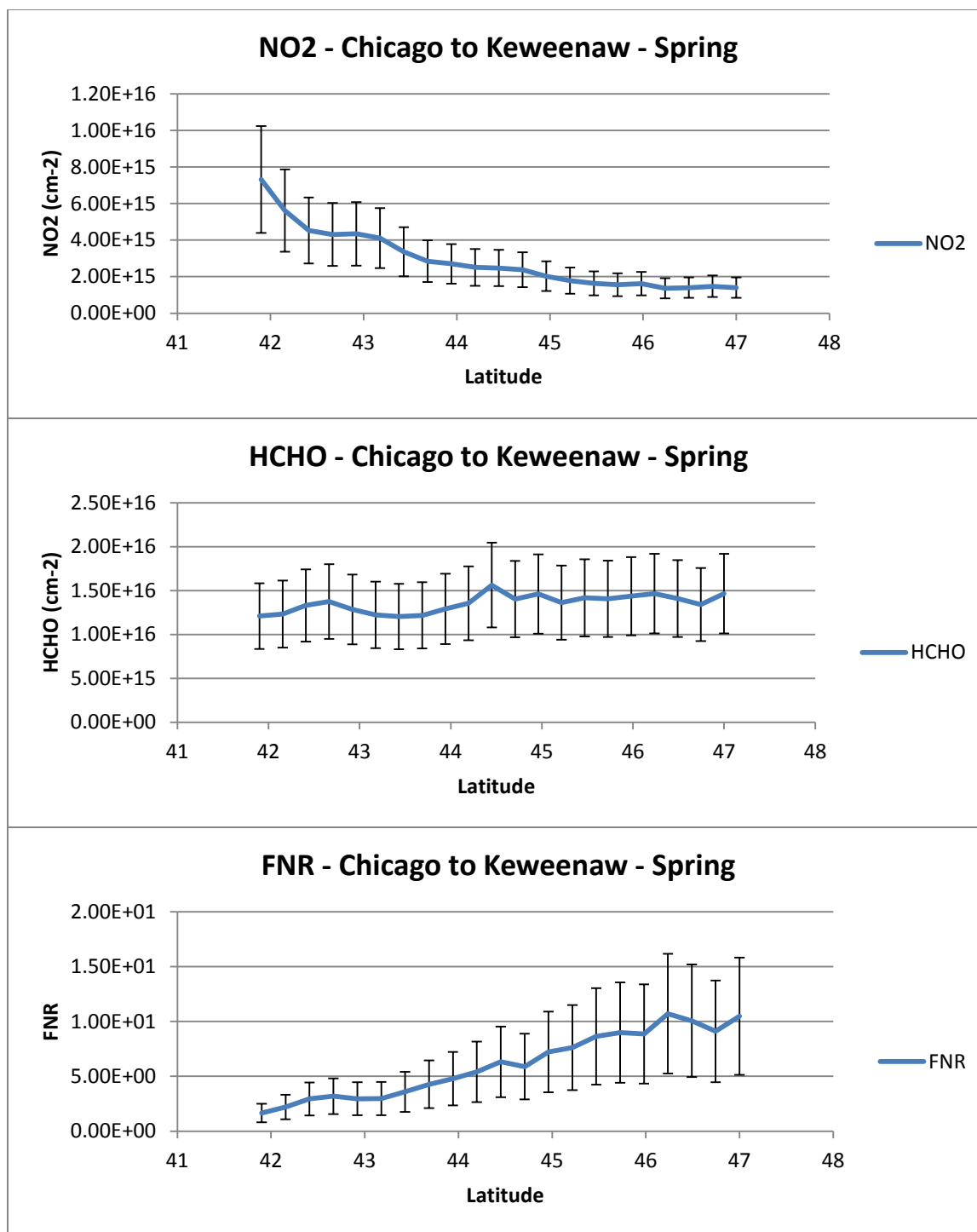


Figure 8: Column densities of (8a, top) NO<sub>2</sub>, (8b, middle) HCHO, and (8c, bottom) FNR during spring.

Analysis of the fall data can be found in Figure 12. From Figure 12a, it can be seen that there is a strong gradient from the lower latitudes to higher latitudes. Taking into

account the error bars, the points corresponding to Chicago are statistically higher than most of the points corresponding to north half of the line which is where the land use changes from cities to small towns; this is similar to the results for spring and summer data. The lowest column density is  $1.71 \times 10^{15} \text{ cm}^{-2}$  at  $47^\circ\text{N}$  which compared to the highest column density of  $7.98 \times 10^{15} \text{ cm}^{-2}$  at  $41.9^\circ\text{N}$  is only 21.4 percent of the highest density. This difference, like with the other seasons, is outside the error bars for both points, albeit a smaller difference by percentage.

The plot of fall HCHO is much the same as the spring and summer HCHO data and shows no significant gradient or difference across the line. Also like the spring and summer, the fall data shows that HCHO is constant along the line with minor changes in the mean column density that are very much within the error bars.

The plot for fall FNR shows a weak gradient from urban to rural with urban areas possessing lower FNR and rural areas possessing higher FNR. Like with the other three seasons, several points further north in the gradient line are significantly higher than the first few points in the urban Chicago area. The lowest FNR is 1.69 at  $41.9^\circ\text{N}$  and the highest FNR is 9.75 at  $46.5^\circ\text{N}$ ; the lowest FNR is 17.3 percent of the highest FNR and the difference is greater than the sum of the error bars. Almost all of the data points have a FNR above 2 which means these regions have  $\text{NO}_2$ -limited  $\text{O}_3$  production. The southernmost point in urban Chicago has a FNR between 1 and 2 which suggests these regions have  $\text{O}_3$  production sensitive to changes in both species. With error potentially pushing it above 2 or below 1, the regime could be  $\text{NO}_x$ -limited or VOC-limited.

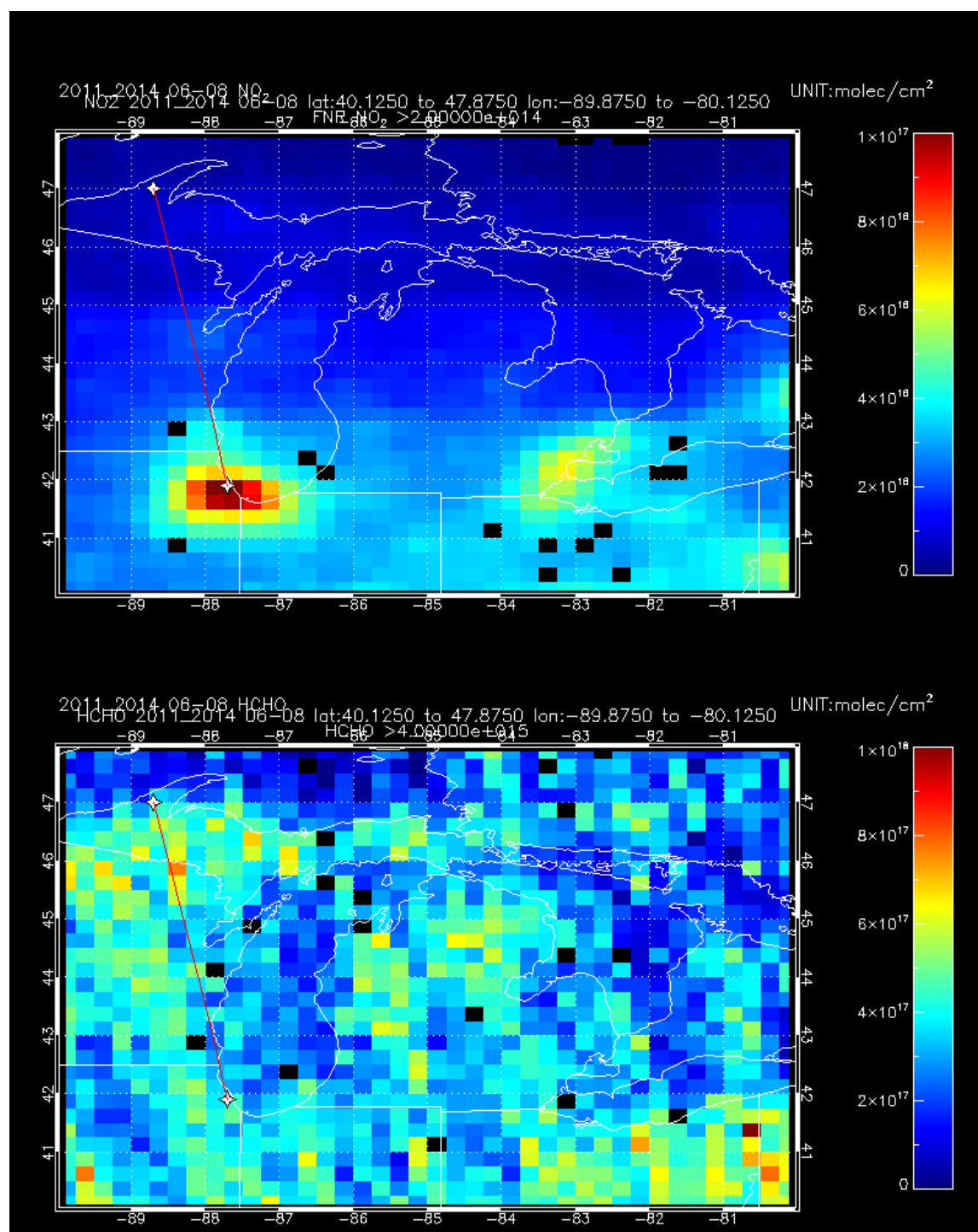


Figure 9: Column densities of (9a, top)  $\text{NO}_2$  and (9b, bottom)  $\text{HCHO}$  from OMI data during summer.

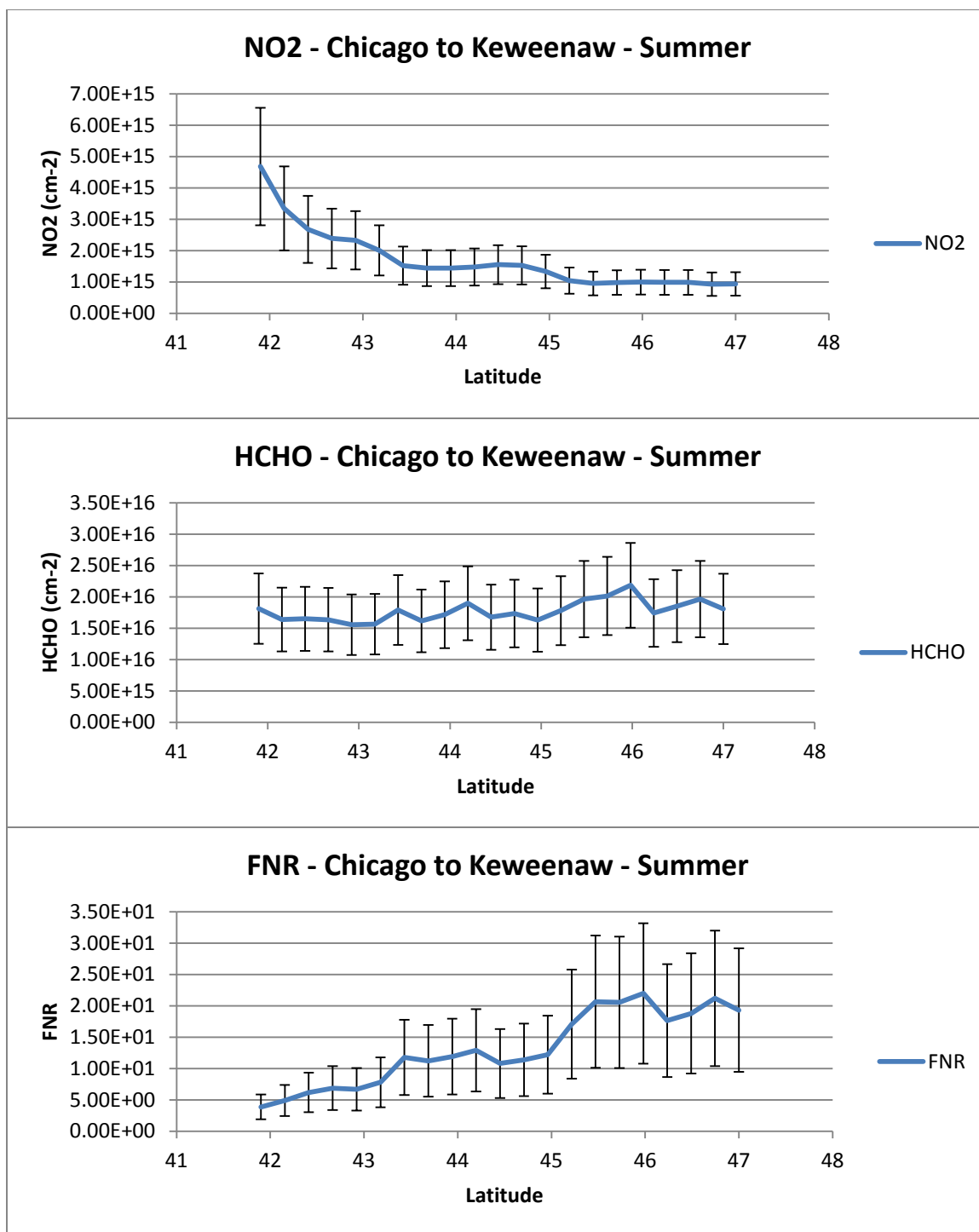


Figure 10: Column densities of (10a, top) NO<sub>2</sub>, (10b, middle) HCHO, and (10c, bottom) FNR during summer.

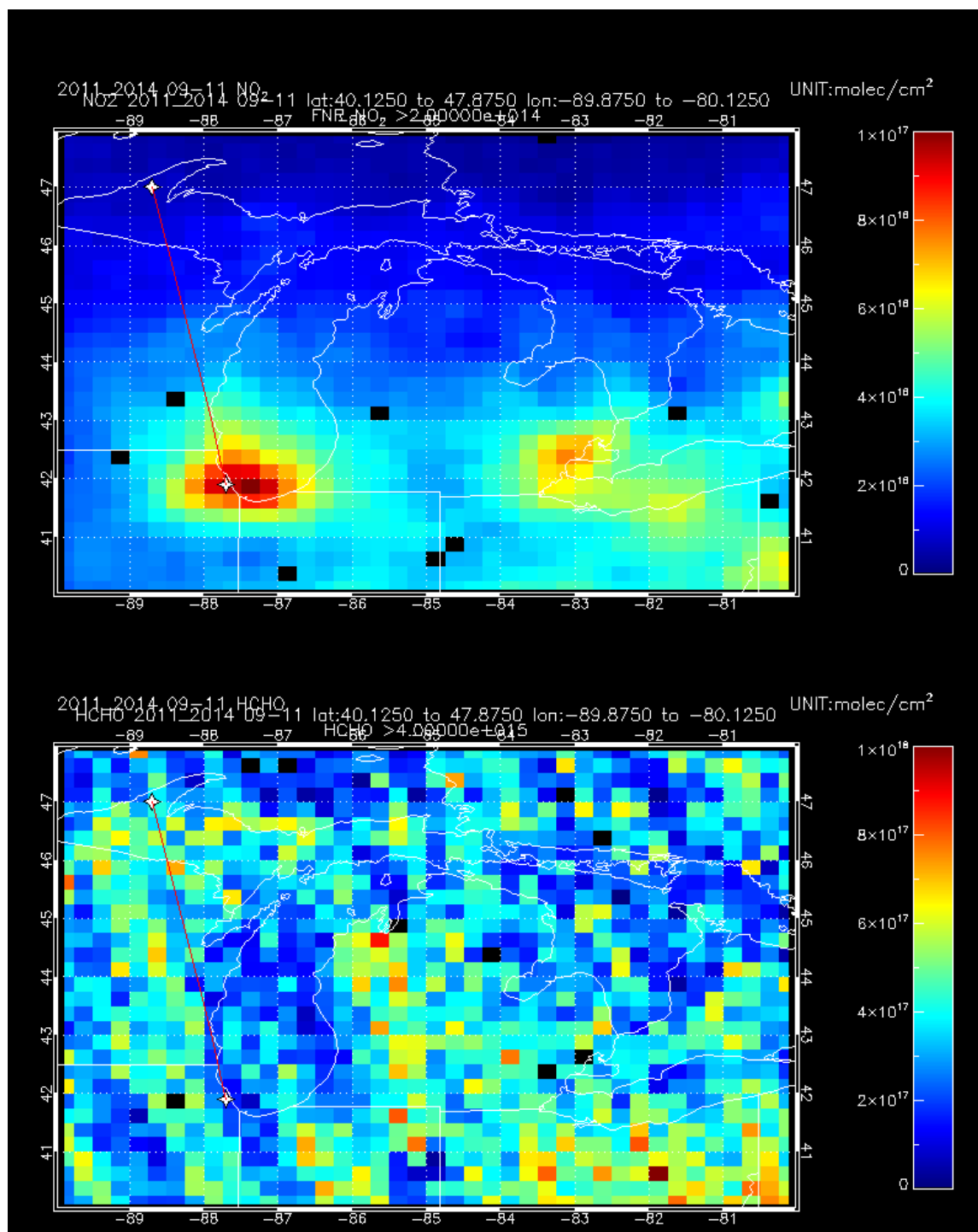


Figure 11: Column densities of (11a, top)  $\text{NO}_2$  and (11b, bottom)  $\text{HCHO}$  from OMI data during fall.

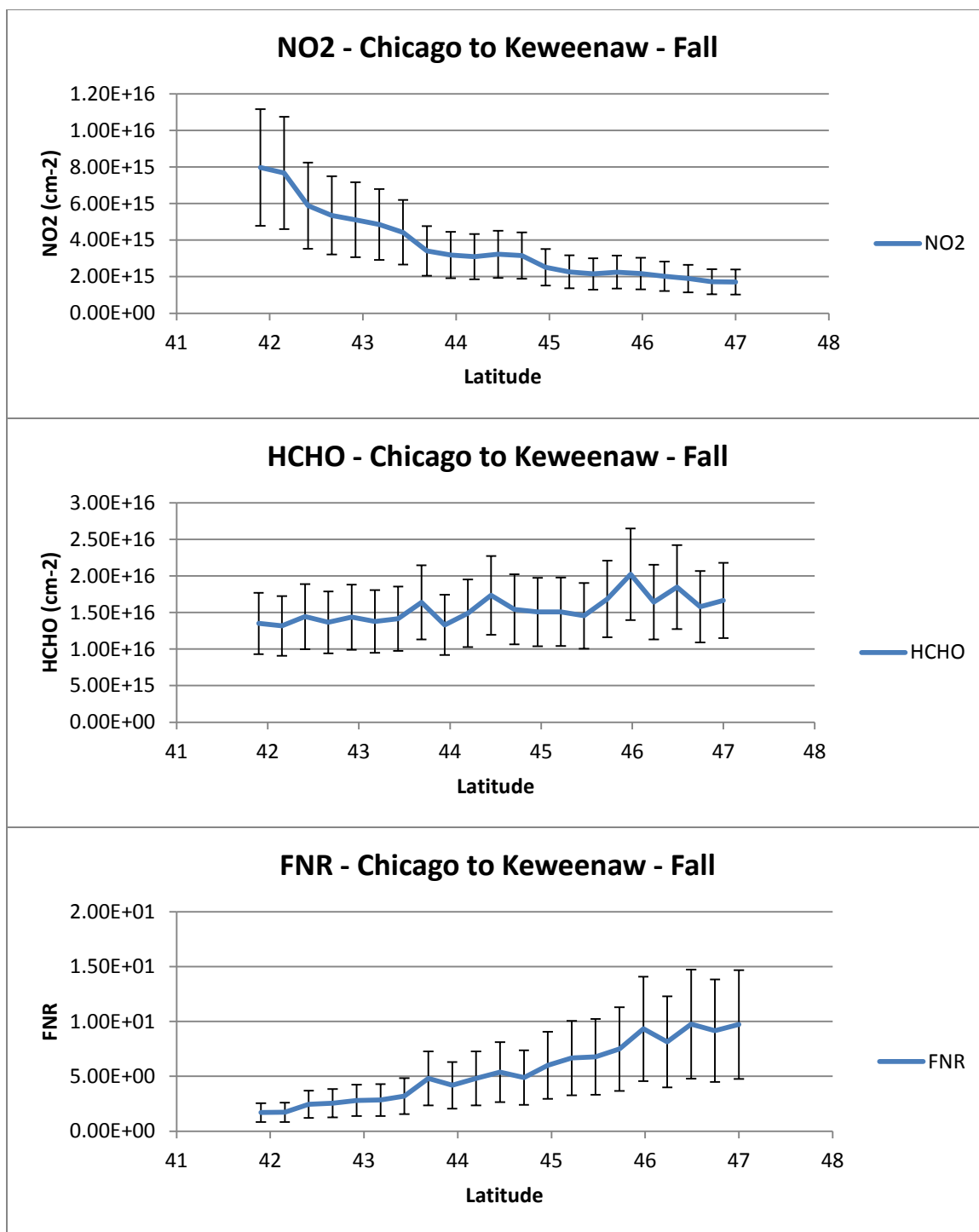


Figure 12: Column densities of NO<sub>2</sub> (12a, top), HCHO (12b, middle), and FNR (12c, bottom) during fall.

Overall, there was a measured gradient of NO<sub>2</sub> column density and FNR between urban and rural areas and the differences between the highest value and lowest value for

each were greater than the error bars in each season. There was no measured gradient for HCHO as the column densities measured were all inside the error bars and not significantly different across the line. Most of the FNR values for the line were above 2 and therefore in the NO<sub>x</sub>-limited regime but there were a few points between 1 and 2 that are in the regime sensitive to both species and a single point in the winter season below 1 that could be in the VOC-limited regime.

### **3.3 Gradient from Detroit to Mackinac Bridge**

The second of the two gradients to be analyzed is between the Detroit metropolitan area (42.4°N, 83.2°W) and the southern end of the Mackinac Bridge just outside of Mackinaw City (45.7°N, 84.7°W). Like the other gradient, the line between these two passes through heavy urban land use with Detroit itself, dense suburban sprawl with Detroit suburbs, smaller cities like Flint and Saginaw, large highways through the center of Michigan, rural northern Michigan towns, and forested land use areas near the tip of the Lower Peninsula. This line should also cover a land use gradient from urban to rural along its length albeit with possible different features. Along the gradient, column densities of NO<sub>2</sub> and HCHO were retrieved every 0.25 degrees of latitude. From these column densities, FNR was calculated for the same latitude intervals. Error bars are included using the error estimates presented in the previous chapter: 40 percent for NO<sub>2</sub> column, 31 percent for HCHO column, and 51 percent FNR from propagation of errors.

As with the other gradient there may be differences between seasons for the column densities and the FNR, the analysis was performed by season. Values for each day's pixel containing the gradient line were compiled across all four years 2011 to 2014 and averaged together to give a single value for column density for each season. For the purposes of this research, winter is considered to be January, February, and December; spring is considered to be March, April, and May; Summer is considered to be June, July, and August; and Fall is considered to be September, October, and November. Thus, the

analysis for winter has all of the days of January, February, and December from 2011, 2012, 2013, and 2014 averaged together at each pixel along the gradient line.

Satellite data for winter can be found in Figure 13 below. The gradient from high NO<sub>2</sub> column densities (yellow color in figure) to low column densities (blue color in figure) appears to correspond with the line between Detroit and the Mackinac Bridge with the high density in urban Detroit and the low densities in the northern Lower Peninsula near the Bridge. There does not seem to be any clear gradient for the HCHO data along the line with some pixels being higher densities (lighter blue) and some pixels being lower densities (darker blue).

Analysis of the winter data can be found in Figure 14. From Figure 14a, it can be seen that there is a gradient from the lower latitudes to higher latitudes. Taking into account the error bars, the points corresponding to Detroit are statistically higher than the points corresponding to rural Michigan nearer to the Bridge. The lowest column density is  $2.63 \times 10^{15} \text{ cm}^{-2}$  at 45.4°N which compared to the highest column density of  $7.78 \times 10^{15} \text{ cm}^{-2}$  at 41.9°N is only 33.8 percent of the highest density. This difference is still outside the error bars for both points even though it is lower than for the other gradient.

The plot of winter HCHO for the second gradient shows no significant gradient or difference across the line. There are points that are higher or lower than others but due to the error bars, there is no significant difference to conclude there is a HCHO gradient. There are a few selected points that are higher or lower than others by a percentage greater than the sum of the error bars.



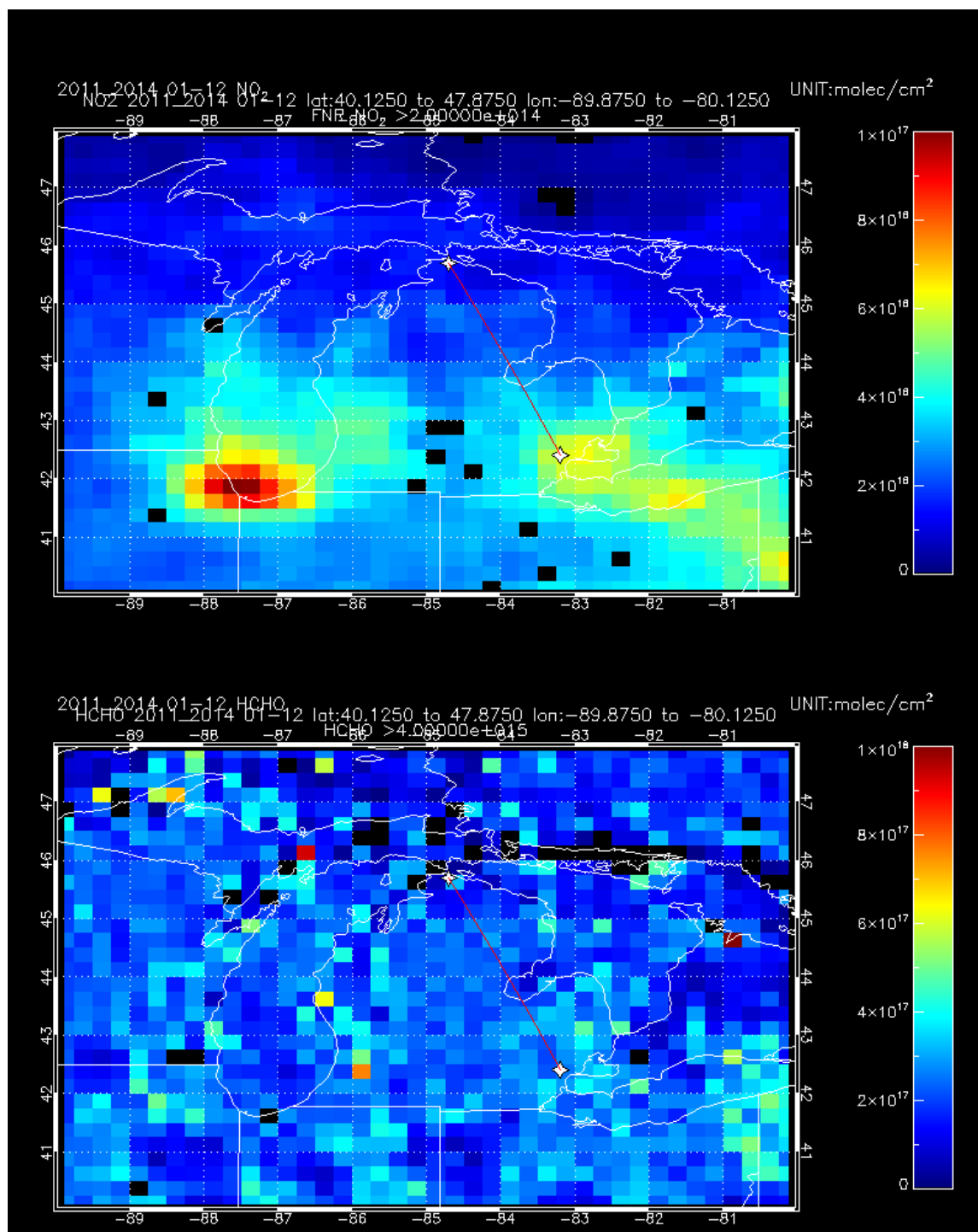


Figure 13: Column densities of (13a, top) NO<sub>2</sub> and (13b, bottom) HCHO from OMI data during winter.

The plot for winter FNR shows a very weak gradient from urban to rural with urban areas possessing lower FNR and rural areas possessing higher FNR. The FNR values for

the two southernmost points, the lowest FNR, are barely statistically lower than the FNR value for the northernmost point, the highest FNR. The lowest FNR is 1.80 at 42.4°N and 42.7°N and the highest FNR is 6.05 at 45.7°N; the lowest FNR is 29.7 percent of the highest FNR and the difference is barely greater than the sum of the error bars. Most of the data points have a FNR above 2 which suggests these regions have NO<sub>x</sub>-limited O<sub>3</sub> production. The lowest points have a FNR between 1 and 2 with taking into account error which suggests these regions have O<sub>3</sub> production sensitive to changes in both species. The error may push these points above 2 giving the regions NO<sub>x</sub>-limited regimes.

Satellite data for spring can be found in Figure 15 below. As with winter, the gradient from high NO<sub>2</sub> column densities to low column densities appears to correspond with the line between Detroit and the Mackinac Bridge with the high density in urban Detroit and the low densities in the northern Lower Peninsula near the Bridge. There does not seem to be any clear gradient for the HCHO data along the line with some pixels being higher densities and some pixels being lower densities.

Analysis of the spring data can be found in Figure 16. From Figure 16a, it can be seen that there is a gradient from the lower latitudes to higher latitudes. Taking into account the error bars, the points corresponding to Detroit are statistically higher than the points corresponding to rural Michigan nearer to the Bridge. The lowest column density is  $1.61 \times 10^{15} \text{ cm}^{-2}$  at 45.7°N which compared to the highest column density of  $5.25 \times 10^{15} \text{ cm}^{-2}$  at 42.4°N is only 30.7 percent of the highest density. This difference is still outside the error bars for both points even though it is again lower than for the other gradient.

The plot of spring HCHO is much the same as the spring HCHO data for the other gradient in that it shows no significant gradient or difference across the line. Also like the other spring data, the spring data for Detroit to Bridge shows that HCHO is constant along the line with minor changes in the mean column density that are very much within the error bars.

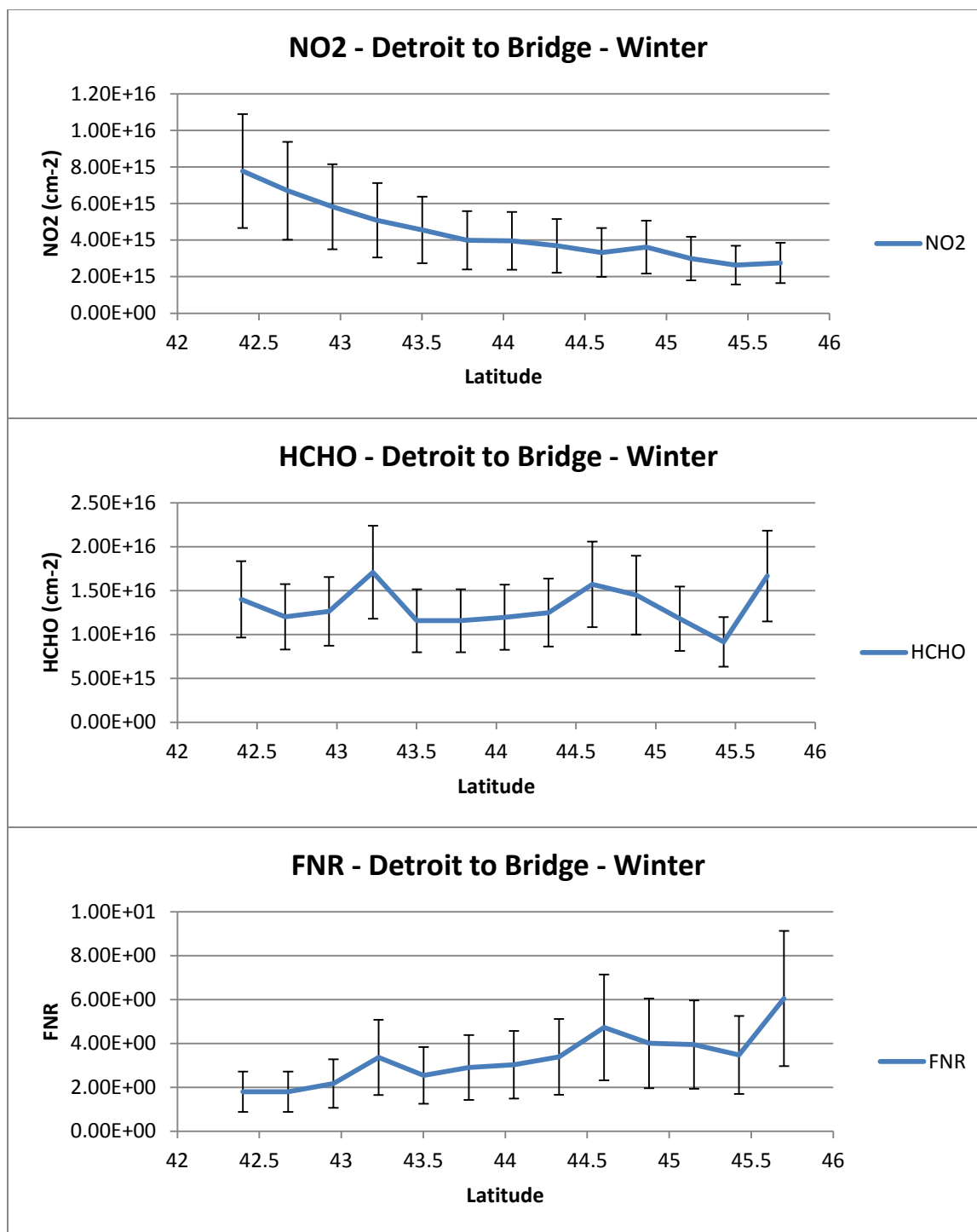


Figure 14: Column densities of (14a, top) NO<sub>2</sub>, (14b, middle) HCHO, and (14c, bottom) FNR during winter.

The plot for spring FNR again shows a very weak gradient from urban to rural with urban areas possessing lower FNR and rural areas possessing higher FNR. The FNR

value for the southernmost point, the lowest FNR, is barely statistically lower than the FNR value for the northernmost point, the highest FNR. The lowest FNR is 2.22 at 42.4°N and the highest FNR is 7.94 at 45.7°N; the lowest FNR is 28.0 percent of the highest FNR and the difference is barely greater than the sum of the error bars. All of the data points have a FNR above 2 which means the whole gradient has NO<sub>x</sub>-limited O<sub>3</sub> production.

Satellite data for summer can be found in Figure 17 below. As with winter and spring, the gradient from high NO<sub>2</sub> column densities to low column densities appears to correspond with the line between Detroit and the Mackinac Bridge with the high density in urban Detroit and the low densities in the northern Lower Peninsula near the Bridge. There does not seem to be any clear gradient for the HCHO data along the line with some pixels being higher densities and some pixels being lower densities.

Analysis of the summer data can be found in Figure 18. From Figure 18a, it can be seen that there is a gradient again from the lower latitudes to higher latitudes. Taking into account the error bars, the points corresponding to Detroit are statistically higher than the points corresponding to rural Michigan nearer to the Bridge. The lowest column density is  $9.35 \times 10^{14} \text{ cm}^{-2}$  at 45.7°N which compared to the highest column density of  $3.12 \times 10^{15} \text{ cm}^{-2}$  at 42.4°N is only 30.0 percent of the highest density. This difference is outside the error bars for both points even though it is again lower than for the gradient from Chicago to Keweenaw.

The plot of summer HCHO is much the same as the spring HCHO data; it shows no significant gradient or difference across the line. Also like the spring data, the summer data for Detroit to Bridge shows that HCHO is constant along the line with minor changes in the mean column density that are very much within the error bars.

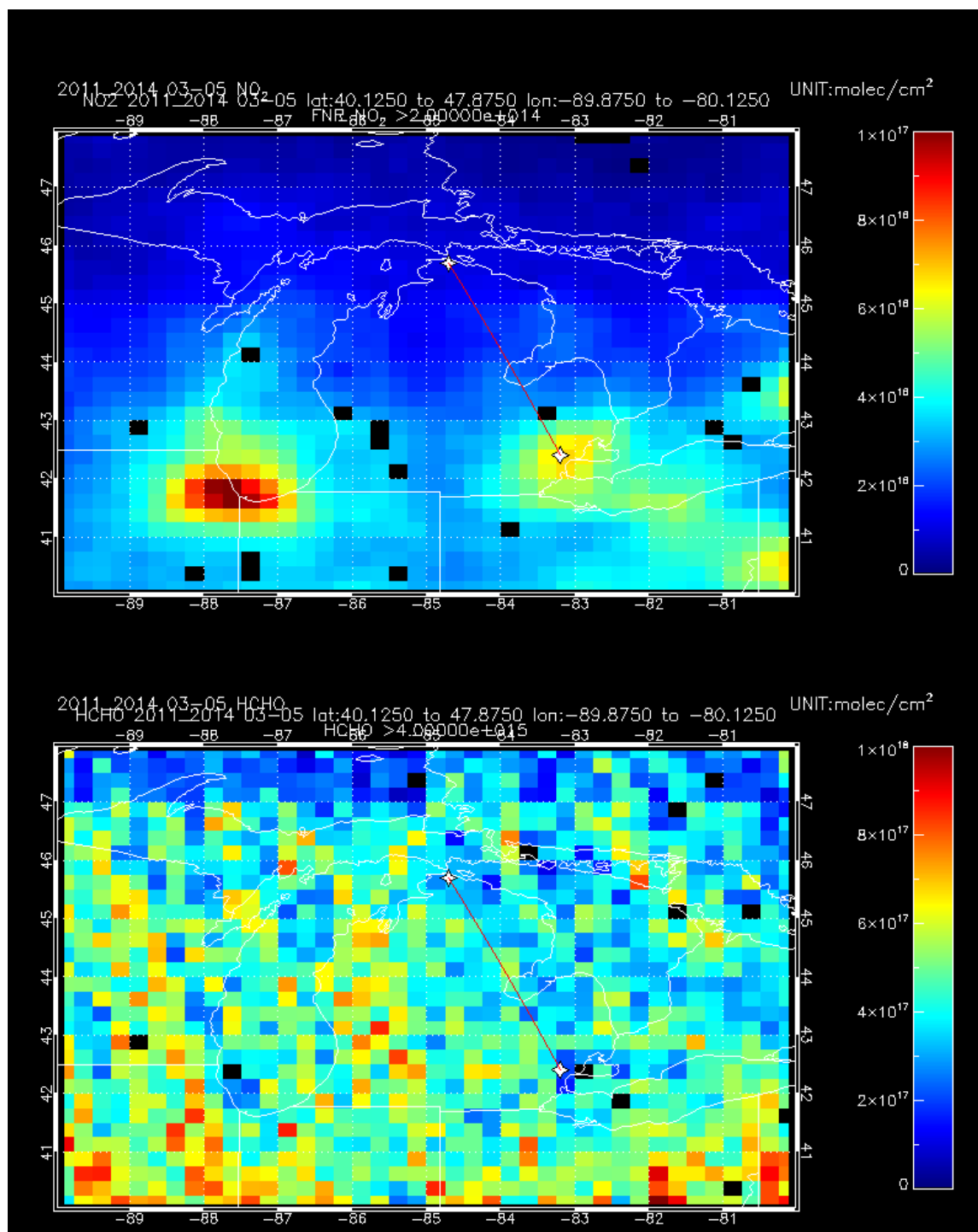


Figure 15: Column densities of (15a, top) NO<sub>2</sub> and (15b, bottom) HCHO from OMI data during spring.

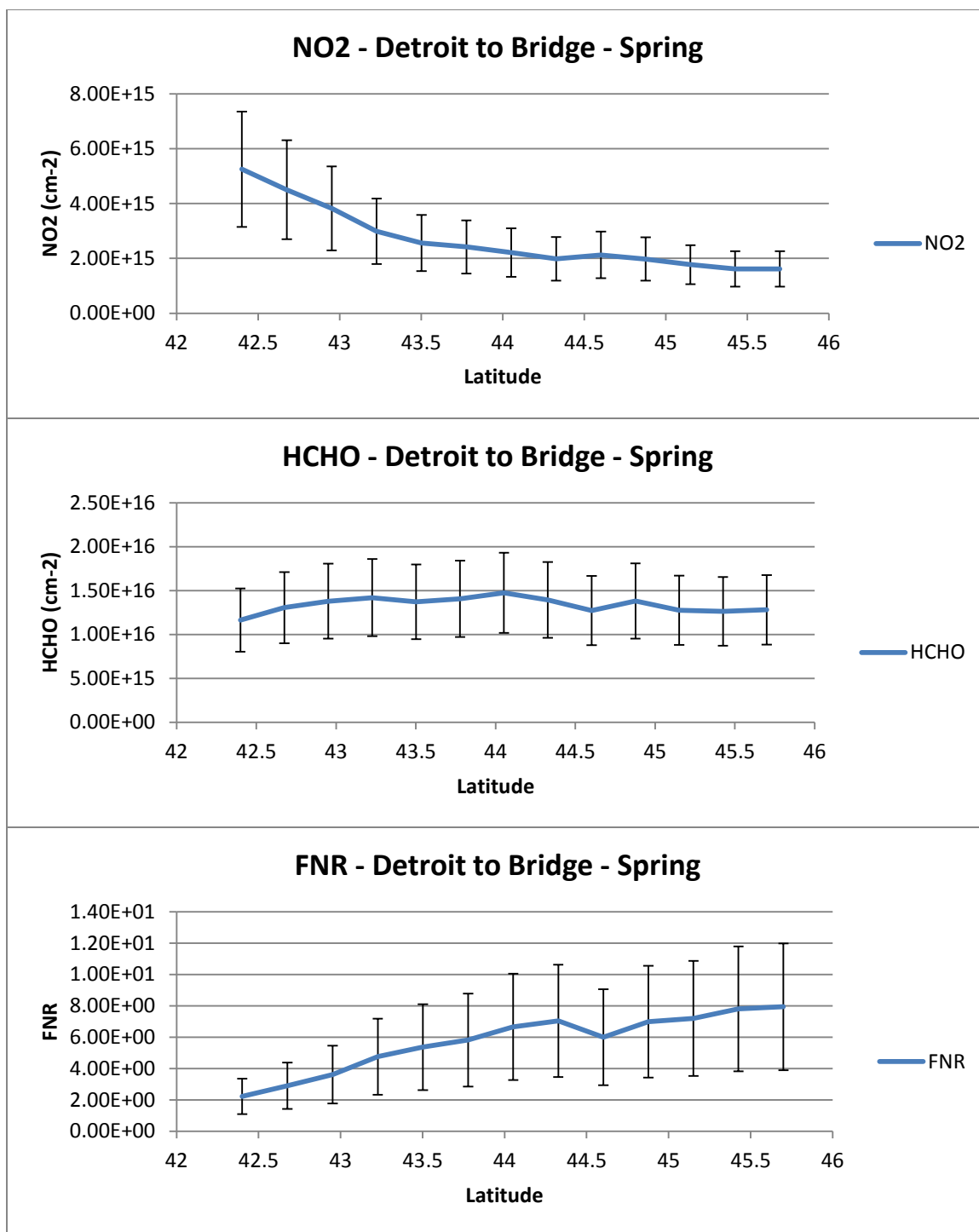


Figure 16: Column densities of (16a, top) NO<sub>2</sub>, (16b, middle) HCHO, and (16c, bottom) FNR during spring.

The plot for summer FNR, like the other seasons, shows a very weak gradient from urban to rural with urban areas possessing lower FNR and rural areas possessing higher FNR. The FNR value for the southernmost point, the lowest FNR, is statistically lower than the FNR value for the northernmost point, the highest FNR. The lowest FNR is 5.64 at 42.4°N and the highest FNR is 20.1 at 45.4°N; the lowest FNR is 28.0 percent of the highest FNR and the difference is greater than the sum of the error bars. All of the data points have a FNR greater than 2 which means the whole gradient has NO<sub>x</sub>-limited O<sub>3</sub> production.

Satellite data for fall can be found in Figure 19 below. As with the other seasons, the gradient from high NO<sub>2</sub> column densities to low column densities appears to correspond with the line between Detroit and the Mackinac Bridge with the high density in urban Detroit and the low densities in the northern Lower Peninsula near the Bridge. There does not seem to be any clear gradient for the HCHO data along the line with some pixels being higher densities and some pixels being lower densities.

Analysis of the fall data can be found in Figure 20. From Figure 20a, it can be seen that there is still a gradient from the lower latitudes to higher latitudes. Taking into account the error bars, the points corresponding to Detroit are still statistically higher than the points corresponding to rural Michigan nearer to the Bridge. The lowest column density is  $2.16 \times 10^{15} \text{ cm}^{-2}$  at 45.4°N which compared to the highest column density of  $6.63 \times 10^{15} \text{ cm}^{-2}$  at 42.4°N is 32.6 percent of the highest density. This difference is outside the error bars for both points.

The plot of fall HCHO is largely the same as the other HCHO data; it shows no significant gradient or difference across the line. Also like the other data, the fall data for Detroit to Bridge shows that HCHO is constant along the line with minor changes in the mean column density that are very much within the error bars.

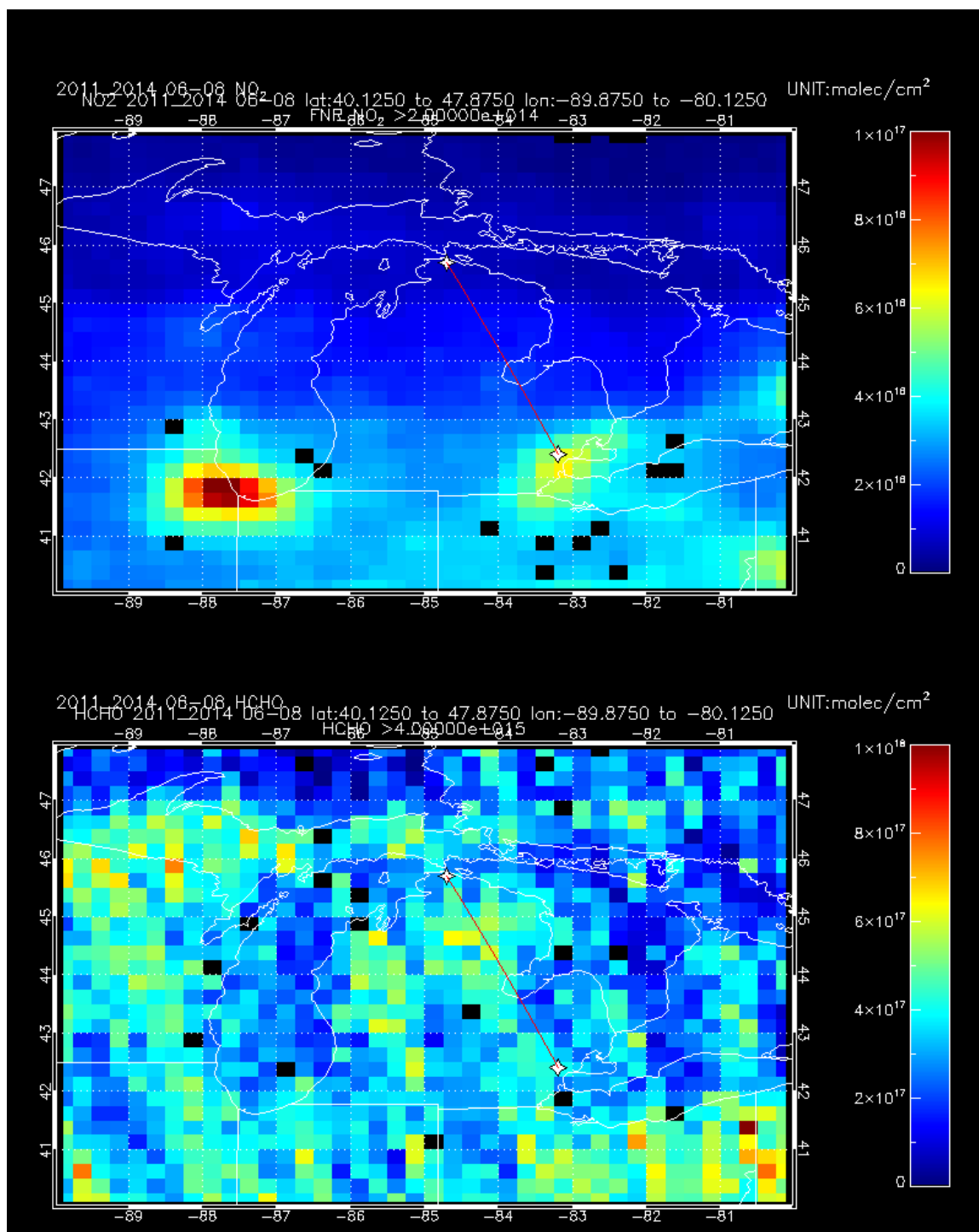


Figure 17: Column densities of (17a, top) NO<sub>2</sub> and (17b, bottom) HCHO from OMI data during summer.



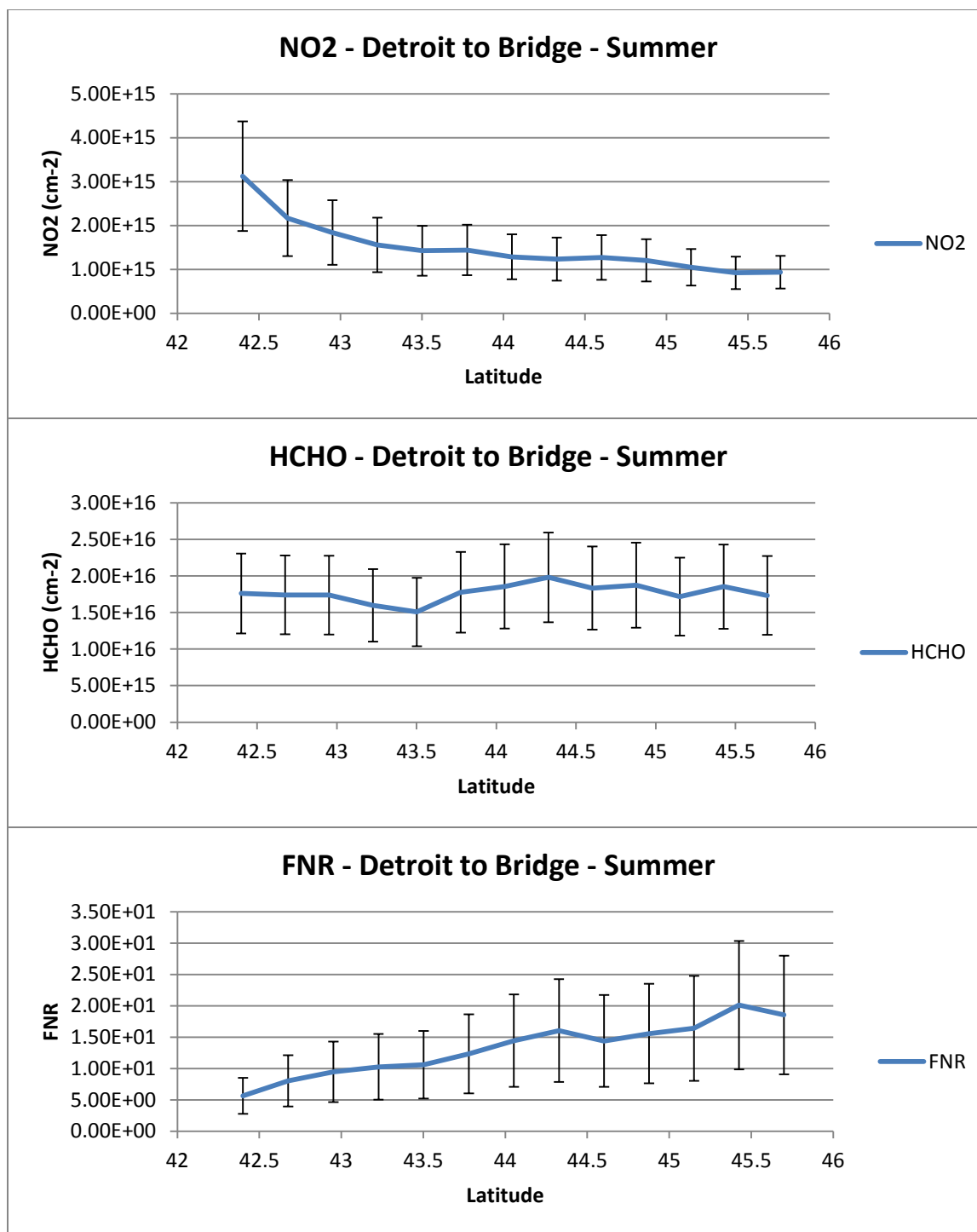


Figure 18: Column densities of (18a, top) NO<sub>2</sub>, (18b, middle) HCHO, and (18c, bottom) FNR during summer.



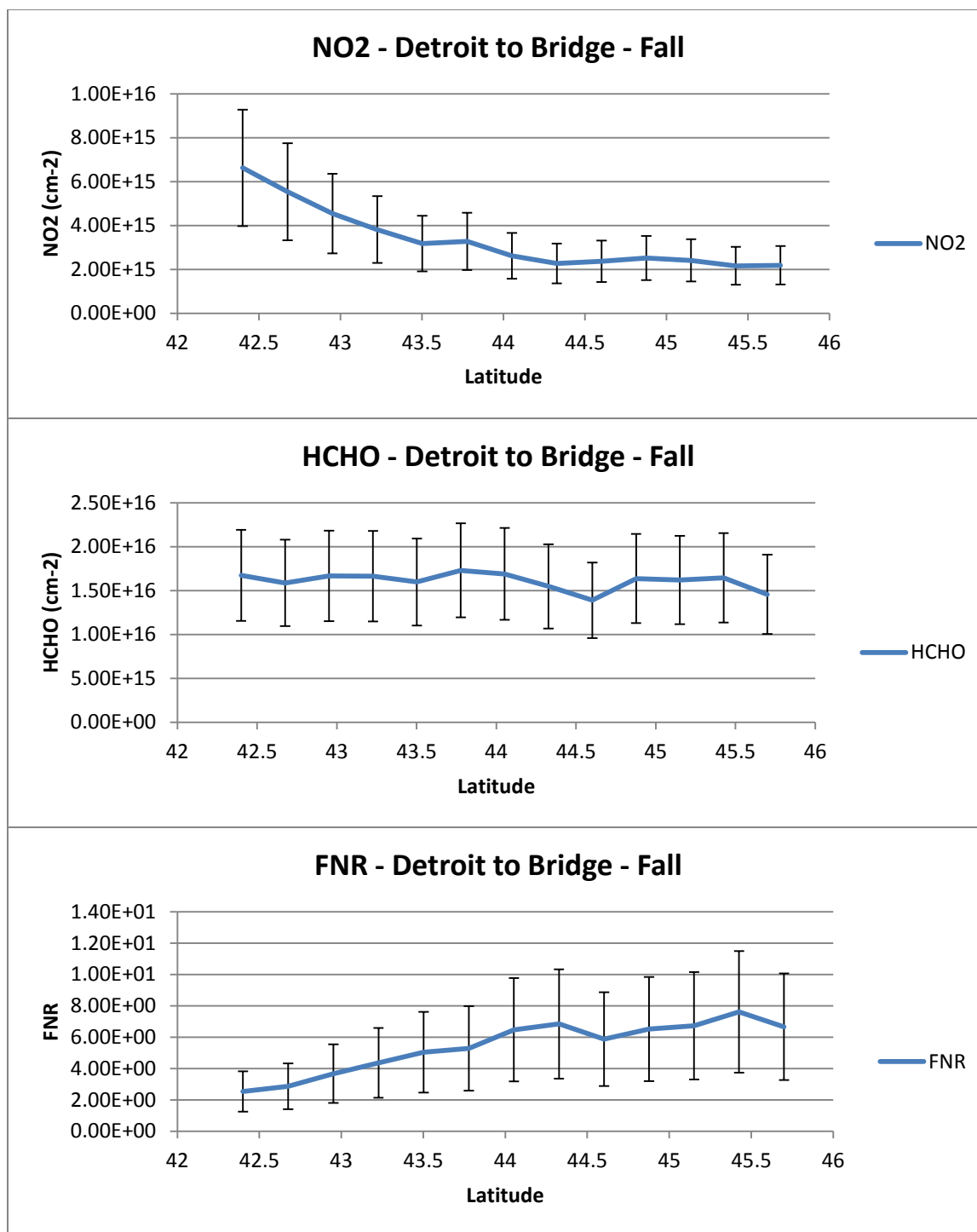


Figure 20: Column densities of (20a, top) NO<sub>2</sub>, (20b, middle) HCHO, and (20c, bottom) FNR during fall.

The plot for fall FNR is however unlike the other seasons as it does not show a mathematically statistical gradient from urban to rural with urban areas possessing lower

FNR and rural areas possessing higher FNR. The plot does show a visual gradient with urban areas low and rural areas high but the lowest FNR and highest FNR have their error bars overlapping; it cannot be concluded that there is a significant difference between the two. Since all of the error bars overlap so while the mean FNR is increasing, there is no significant change that can be concluded. The lowest FNR is 2.52 at 42.4°N and the highest FNR is 7.61 at 45.4°N; the lowest FNR is 33.1 percent of the highest FNR. This difference is not greater than the sum of the error bars. The bottom of the error bar for the highest FNR is at 3.73 while the top of the error bar for the lowest FNR is 3.81. All of the data points have a FNR greater than 2 which means the whole gradient has NO<sub>x</sub>-limited O<sub>3</sub> production.

Overall, there was a measured gradient of NO<sub>2</sub> column density and FNR between urban and rural areas and the differences between the highest value and lowest value for each were greater than the error bars in each season except for fall which did not have a significant gradient for FNR. There was no measured gradient for HCHO as the column densities measured were all inside the error bars and not significantly different across the line. Most of the FNR values for the line were above 2 and therefore in the NO<sub>x</sub>-limited regime but there were a few points between 1 and 2 that are in the regime sensitive to both species.

### **3.4 Seasonal Dependence of FNR**

Mean FNR values for each season in Chicago, Green Bay, Detroit, the middle of the Keweenaw Peninsula, and near the Mackinac Bridge can be found in Table 2. FNR values for all sites are highest in the summer months and lowest in the winter months. Spring and fall appear to have similar FNR values at each site. Difference between winter and summer for all sites is significant to conclude that there is a seasonal dependence in FNR.

Differences in FNR between locations (Table 2) show that cities like Chicago and Detroit have lower FNR values in each season than rural areas like the Keweenaw and the Mackinac. Green Bay is in between the cities and the rural areas with its FNR values.

	<b>Chicago</b>	<b>Keweenaw</b>	<b>Green Bay</b>	<b>Detroit</b>	<b>Mackinac</b>
<b>Winter</b>	0.930	2.266	2.838	1.800	6.050
<b>Fall</b>	1.694	9.721	5.381	2.525	6.663
<b>Summer</b>	3.872	19.313	10.804	5.639	18.549
<b>Spring</b>	1.653	10.486	6.317	2.218	7.938

Table 2: Mean FNR values for five locations in the Great Lakes region for each season.

## 4. Discussion

### 4.1 Sensitivity Analysis

In the sensitivity analyses conducted at the four sites in a line up the lakeshore of Lake Michigan, it is demonstrated that OMI NO<sub>2</sub> retrievals and ground-instrument retrievals are in rough agreement in showing annual and weekly trends. At the Chicago site, OMI and ground instrument both have high retrievals in the winter and low in the summer. Both have uniform retrievals across the week with a slight dip on the weekend. It can be safely assumed that OMI is sensitive to the changes at the surface across the year and the week in the Chicago region and for urban regions. At the Milwaukee site, OMI and ground instruments also have high retrievals in the winter and low in the summer. Retrievals across the week are uniform between the two instruments and both dip over the weekend. As with the Chicago site, it can be assumed that OMI is sensitive to surface changes in the region and land use type. The Manitowoc site is different. The ground instrument at the site only retrieved mixing ratios for five out of the twelve months of the year while OMI has retrieved columns for all twelve months. There is insufficient data in the annual analysis to determine the satellite instrument's sensitivity to ground chemistry. The weekly analysis shows strong agreement between the two instruments. At the Potawatomi site, OMI and ground instruments agree with each other with changes at the ground with the exception of the local maximum in May and June present in the ground instrument. This local maximum is consistent with profiles of mixing ratio for the individual years. It is unknown the source of this local maximum and why OMI did not observe similar changes.

From these analyses, it can be assumed that OMI is sensitive to ground changes even in rural areas and can be used for further research in both urban and rural areas. The following sections regarding NO<sub>2</sub> gradients, HCHO gradients, FNR gradients, and O<sub>3</sub> production regimes using OMI is made possible by this sensitivity analysis.

## 4.2 NO<sub>2</sub> Gradients

For all four seasons for both gradient lines, a NO<sub>2</sub> gradient was seen. In each case, the highest column densities were significantly higher than the lowest column densities by more than the sum of the error bars. Urban areas such as Chicago and Detroit were shown to have a higher column density of NO<sub>2</sub> than rural areas in northern Wisconsin and northern Michigan. This is a confirmation of the hypothesized gradients between urban and rural in that the urban regions with high expected concentrations of NO<sub>2</sub> had high concentrations of NO<sub>2</sub>. Rural areas, with low expected concentrations had lower concentrations. Due to the lifetime of NO<sub>x</sub> in the atmosphere, long-range transport of NO<sub>2</sub> on this spatial scale was not expected and the rural areas remained low as expected despite potentially being downwind of urban regions. The distance between regions is also likely not large enough for NO<sub>2</sub> to be incorporated into reservoir species and lofted high in the atmosphere for long range transport.

Contrary to expectation, there are no smaller increases or decreases present due to transition to and from smaller cities and rural areas. For example, the column density over Green Bay is not significantly higher than the column density over the Keweenaw Peninsula. These smaller cities should be significant enough sources of NO<sub>2</sub> in theory to be seen in the gradient but this has not been seen in the analysis.

In terms of seasonal cycles, NO<sub>2</sub> is highest in winter and lowest in summer for both paths. This fits with expectations based on previous studies and based on atmospheric chemistry of the compound. In the Great Lakes region, there is more emission of NO<sub>x</sub> due to increased combustion from heating and power plants. Destruction of NO<sub>x</sub> is also lessened in the winter due to colder temperatures and reduced sunlight.

This research shows that even with the inherent error of OMI, gradients can be measured between large cities and rural areas. While a quick visual look at the satellite

imagery may indicate a possible gradient, analysis of the column densities and errors was needed to confirm a statistically significant gradient. OMI does not seem to be precise enough to measure smaller gradients than between major cities and rural areas though.

### **4.3 HCHO Gradients**

HCHO gradients were not seen along the gradient lines across the analysis. Small variations were seen but none were significantly higher than the error bars. This confirms the hypothesis that there will be no significant difference in HCHO column density between urban and rural areas along the gradient. However, there is no way to know if the lack of gradient is due to limitations of the instrument or a true lack of gradient in HCHO column densities. Uniformity in HCHO can be expected because the sources are constant in both urban and rural areas and no transport can be expected because of the short lifetime.

HCHO is found to have higher measured concentrations in summer than in winter; this is expected from previous studies and the temperature dependence of VOC production. The fact that HCHO changes with seasons but not along the path indicates that OMI data is capable of measuring HCHO concentrations in the rural areas rather than just reporting instrument noise.

Because OMI is unable to measure any gradient in HCHO due to the inherent errors of the instrument as any gradient present in the atmosphere should be less than the errors of the instrument, an instrument with a very high sensitivity would be needed to measure any minute gradients that may be present in HCHO. In theory, a very strong gradient of column density for HCHO between two regions may be detectable but for column densities present in the region of interest, OMI is unable to measure a significant gradient. This is consistent with the HCHO data from Duncan et al [2010] where it is shown that significant gradients require a greater distance using the OMI instrument; HCHO values are too uniform at the scale of the Great Lakes region.

### **4.4 FNR Gradients**

FNR gradients were seen in all cases except for the fall data between Detroit and the Bridge. FNR was significantly lower in the urban areas than in the rural areas with the difference exceeding the error bars. This gives evidence that OMI can be used to measure gradients in FNR for sufficiently strong gradients between different land use types. Gradients that are much shallower such as between small towns and rural or between a city and its suburban area would not be able to be resolved using OMI.

Some of the rural areas measured have FNR values that are unambiguously above 2, putting them in the NO<sub>2</sub>-limited regime of O<sub>3</sub> production. The deep urban areas often have FNR values between 1 and 2, putting them in a neutral regime sensitive to both species. A few points in urban areas have mean FNR values below 1, putting them in VOC-limited regimes. Errors inherent in the instrument, being 51 percent of the mean FNR, lead to ambiguity about the true FNR value for the pixels however so in many cases, the ozone production chemistry is unknown using OMI. With errors being that high, in order to definitively say that the FNR is below 1 and in the VOC-limited regime, the mean FNR would have to be 0.662 as the top of the error bar would be at 1. The whole range of values taking into account the errors would be below 1 and OMI can confirm the VOC-limited regime.

For OMI to confirm the pixel is in the NO<sub>2</sub>-limited regime, the bottom of the error bar would have to be at 2 which means the mean FNR value would have to be 4.082 so that the 51 percent error would bring it down to 2. There is no FNR mean value that will have its error bars remain between 1 and 2 as the mean value with 2 at the higher bound of its error will have a lower bound below 1. The FNR value that has its lower bound at 1 is greater than 2.

OMI is then able to determine the O<sub>3</sub> production regime of a region or pixel if the measured FNR is above 4.082 (NO<sub>x</sub>-limited regime) or below 0.662 (VOC-limited regime). The regime of the region is undeterminable with OMI data if the FNR is anywhere between these two values and a dual sensitivity regime is undeterminable with OMI data. Because of this, OMI is not a powerful instrument to determine production regime except in cases of extremes. There are still some regions undeniably in the NO<sub>x</sub>-limited regime in the rural regions that OMI has been able to determine.



Being able to determine the O<sub>3</sub> production regime of the region can also help understand how additional emission and transport will affect the region. Since many of the rural areas are found to have significantly high FNR values to be in the NO<sub>x</sub>-limited regime, the region's O<sub>3</sub> production is sensitive to changes in NO<sub>x</sub>. This means that if a new source of NO<sub>x</sub> is introduced to the region such as a new industrial building, power plant, or large wildfire or a plume of NO<sub>x</sub> is transported downwind from source to rural region, the O<sub>3</sub> concentration will increase. If a source of NO<sub>x</sub> is removed or downwind transport is removed, the O<sub>3</sub> concentration will decrease. However, changes in VOCs will not change the O<sub>3</sub> concentration much. This is important to consider when drafting regulations and policies for the region as well as understanding the big picture of O<sub>3</sub> production in the greater region.

For urban regions with FNR values low enough to be classified to be in VOC-limited regimes, the opposite is true. The O<sub>3</sub> production is sensitive to changes in VOCs and less sensitive to changes in NO<sub>2</sub>. New sources of VOCs or transport of VOCs from other regions will lead to increases in O<sub>3</sub> production. Removal of sources or transport will lead to a decrease. Changes in NO<sub>x</sub> will not lead to significant changes in O<sub>3</sub> production. This is important as well for regulations, policies, and greater understanding, especially since many regulations and policies in the past have sought to control the NO<sub>x</sub> concentrations through emission controls. This reduction in NO<sub>x</sub> concentration will not reduce O<sub>3</sub> production in the low FNR urban region – VOC controls are needed for that – but it will reduce O<sub>3</sub> production in downwind rural regions with high FNR values.

FNR values have seasonal dependency, being higher in summer than in winter. This is most likely due to temperature dependency for HCHO and seasonal dependency for both HCHO and NO<sub>2</sub>. Since NO<sub>2</sub> is higher in winter and HCHO is higher in summer as a result of warmer temperatures, FNR is higher in summer and lower in winter.

Overall, in the Great Lakes region there appears to be much more area in NO<sub>x</sub>-limited regime than VOC-limited regime. This means that the O<sub>3</sub> production in the Great Lakes region increases and decreases with changes in NO<sub>x</sub> with the exception of the heavy urban areas and changes in VOC concentrations will not change the O<sub>3</sub> production much.

Controls and regulations on pollution and emission to control  $O_3$  will be best placed on  $NO_x$  sources in the region.

These findings are called into question by OMI being unable to find a gradient in HCHO. Because FNR is a ratio of HCHO to  $NO_2$ , both concentrations must be trusted in order to make claims about the FNR values. As it is not known whether the lack of gradient is due to uniformity in HCHO along the path or inability to retrieve HCHO data since both scenarios would appear the same, it cannot be determined that OMI can detect HCHO and therefore it cannot be determined that OMI can measure FNR along the path. If this is true, FNR is only dependent on the concentrations of  $NO_2$  and serves as an inverse of  $NO_2$  concentration. While the data appears to show gradients in FNR, it may just be a second way to show a change in  $NO_2$  along the path and provide no information as to the  $O_3$  chemistry regime. Because of this, it may not be possible to say with certainty that there is a significant gradient in FNR without having improved HCHO retrievals or decreased error.

## **5. Conclusion**

This research has shown that OMI is a useful instrument for retrieving  $NO_2$  column densities, HCHO column densities, and FNR in urban and rural regions. OMI is sensitive to changes in gas concentrations at the surface as demonstrated in the comparison analyses. It can retrieve gradients from urban to rural and function as a remote sensing instrument for regions unsuitable for year-round ground-based instruments. Between major urban centers and rural areas in the northern Great Lakes regions, there exist gradients in  $NO_2$  and FNR but not HCHO. Furthermore, regions with definite  $O_3$  production chemistry regimes were identified. Even along the gradients before a significant difference is retrieved, there is visual indication of a gradient. Along these visual gradients, there is a percentage difference between high and low that is less than that of significance. FNR values are highest in rural areas and during the summer months. Because FNR is higher during summer months,  $O_3$  production is more sensitive to changes in  $NO_x$  in the atmosphere and since  $NO_x$  is a very common emission from

both natural and anthropogenic sources,  $O_3$  production could lead to dangerous concentrations of  $O_3$  in the region. Higher FNR in rural areas also means the  $O_3$  production has an increased sensitivity to  $NO_x$  emissions. While there may be fewer sources of  $NO_x$  emissions in rural areas, this production regime could cause harmful spikes in  $O_3$  concentrations when a plume of  $NO_x$  enters the region from an upwind source; in this way urban emissions can be dangerous to downwind rural areas.

Flaws with the instrument include large errors. With  $NO_2$  errors at 40 percent and HCHO errors at 31 percent, subtle gradients are almost impossible to distinguish. Only major gradients between urban areas and rural areas are significant enough for OMI analysis. Furthermore, the propagation of errors makes the error in FNR up to 51 percent; this means FNR gradients must also be large in order to be significant enough for OMI to distinguish between regimes. This means that OMI may only be useful for studying FNR gradients and  $O_3$  production regimes on a super-regional scale or in cases where there is a strong or weak local source of  $NO_2$  or HCHO so that there is a strong enough gradient between low FNR and high FNR. The large error also makes the FNR values needed to definitively classify a region as being in the VOC-limited regime or the  $NO_x$ -limited regime very low or very high. Improvement of errors should allow for better classification of gradients, especially where there is a visual gradient but not currently a mathematical gradient. Future research with the OMI data product will need a reduction in errors from either the instrument itself or the data processing method before OMI can be used for analysis of finer gradients.

As part of the errors present are due to non-systematic sources such as fitting errors and instrumental errors, the error bars can theoretically be reduced by averaging all the data points for a given pixel across years of data. Errors can be reduced using the square root of the number of data points used to obtain the average value. Too much reduction in errors may be an incorrect approach if there are systematic errors that cannot be removed with averaging so careful application of error reduction techniques such as using the square root of the number of data points is important.

Future research should be directed towards the analysis of additional gradients in the Great Lakes region and beyond using OMI, more comparison analysis to ground

instruments, investigation of trends in rural areas in the Great Lakes region, and determining additional uses for OMI in rural areas. Additional gradients will likely be from other major urban areas to rural areas and between two major urban areas. Comparison analysis will seek to determine if results are consistent among different rural areas. Investigation of trends will be supplemental to existing research using OMI to fill in the gaps in rural regions that other literature has not covered. Since OMI is now proven to be suitable for rural region investigation, these trends can be analyzed using OMI.

## List of References

- Abbot D, Palmer P, Martin R, Chance K, Jacob D, and Guenther A. "Seasonal and interannual variability of North American isoprene emissions as determined by formaldehyde column measurements from space." *Geophysical Research Letters*. 30, 17, 1886. (2003).
- Atkinson R and Arey J. "Atmospheric Degradation of Volatile Organic Compounds." *Chem. Rev.* 103, 4605-4638. (2003).
- Balzani Lööv J, Alföldy B, Beecken J, Berg N, Berkhout A, Duyzer J, Gast L, Hjorth J, Jalkanen J-P, Laglet F, Mellqvist J, Prata F, van der Hoff G, Westrate H, Swart D, and Borowiak A. "Field test of available methods to measure remotely SO<sub>2</sub> and NO<sub>x</sub> emissions from ships." *Atmos. Meas. Tech. Discuss.* 6, 9735-9782. (2013).
- Beecken J, Mellqvist J, Salo K, Ekholm J, and Jalkanen J-P. "Airborne emission measurements of SO<sub>2</sub>, NO<sub>x</sub>, and particles from individual ships using sniffer technique." *Atmos. Meas. Tech. Discuss.* 6, 10617-10851. (2013).
- Berg N, Mellqvist J, Jalkanen J-P, and Balzani J. "Ship emissions of SO<sub>2</sub> and NO<sub>2</sub>: DOAS measurements from airborne platforms." *Atmos. Meas. Tech.* 5, 1085-1098. (2012).
- Boeke N, Marshall J, Alvarez S, Chance K, Fried A, Kurosu T, Rappengluck B, Richter D, Walega J, Weibring P, Millet D. "Formaldehyde columns from the Ozone Monitoring Instrument: Urban versus background levels and evaluation using aircraft data and a global model." *Journal of Geophysical Research*. 116, D05303. (2011).
- Boersma K, Eskes H, Veefkind J, Brinksma E, van der A R, Sneep M, van den Oord G, Levelt P, Stammes P, Gleason J, Bucsela E. "Near-real time retrieval of tropospheric NO<sub>2</sub> from OMI." *Atmos. Chem. Phys.* 7, 2103-2118. (2007).
- Bucsela E, Celarier E, Wenig M, Gleason J, Veefkind J, Boersma K, and Brinksma E. "Algorithm for NO<sub>2</sub> Vertical Column Retrieval From the Ozone Monitoring Instrument." *IEEE Transactions on Geoscience and Remote Sensing*. Vol 44, No 5. (2006)
- Carter W. "Development of Ozone Reactivity Scales for Volatile Organic Compounds." *Journal of the Air and Water Management Association*. 44, 881-899. (1994).

- Chance K, Palmer P, Spurr R, Martin R, Kurosu T, and Jacob D. “Satellite observations of formaldehyde over North America from GOME.” *Geophysical Research Letters*. 27, 21, 3461-3464. (2000).
- Dalsøren S, Samset B, Myhre G, Corbett J, Minjares R, Lack D, and Fuglestad J. “Environmental impacts of shipping in 2030 with a particular focus on the Arctic region.” *Atmos. Chem. Phys.* 13, 1941-1955. (2013).
- Duncan B, Prados A, Lamsal L, Liu Y, Streets D, Gupta P, Hilsenrath E, Kahn R, Nielsen J, Beyersdorf A, Burton S, Fiore A, Fishman J, Henze D, Hostetler C, Krotkov N, Lee P, Lin M, Pawson S, Pfister G, Pickering K, Pierce R, Yoshida Y, Ziemba L. “Satellite data of atmospheric pollution for U.S. air quality applications: Examples of applications, summary of data end-user resources, answers to FAQs, and common mistakes to avoid.” *Atmospheric Environment*. 94, 647-662. (2014).
- Duncan B, Yoshida Y, Retscher C, Pickering K, Celarier E. “The Sensitivity of U.S. Surface Ozone Formation to NO<sub>x</sub> and VOCs as Viewed From Space.” *Presentation at 8<sup>th</sup> Annual CMAS Conference*. (2009).
- Duncan B, Yoshida Y, Olson J, Sillman S, Martin R, Lamsal L, Hu Y, Pickering K, Retscher C, Allen D, and Crawford J. “Application of OMI observations to a space-based indicator of NO<sub>x</sub> and VOC controls on surface ozone formation.” *Atmospheric Environment*. 44, 2213-2223. (2010).
- Durant J, Ash C, Wood E, Herndon S, Jayne J, Knighton W, Canagaratna M, Trull J, Brugge D, Zamore W, and Kolb C. “Short-term variation in near-highway air pollutant gradients on a winter morning.” *Atmos. Chem. Phys.* 10, 8341-8352. (2010).
- Fioletov V, McLinden C, Krotkov N, Moran M, and Yang K. “Estimation of SO<sub>2</sub> emission using OMI retrievals.” *Geophysical Research Letters*. Vol. 38, L21811 (2011).
- Frey H, Unal A, Roupail N, and Colyar J. “On-road measurement of vehicle tailpipe emissions using a portable instrument.” *Journal of the Air & Waste Management Association*. 53:8, 992-1002. (2003).

- Frins E, Ibrahim O, Casaballe N, Osorio M, Arismendi F, Wagner T, and Platt U. “Ground based measurements of SO<sub>2</sub> and NO<sub>2</sub> emissions from the oil refinery ‘la Teja’ in Montevideo city.” *Journal of Physics: Conference Series*. 274 (2011).
- Gielen C, Van Roozendaal M, Hendrick F, Pinardi G, Vlemmix T, De Bock V, De Backer H, Fayt C, Hermans C, Gillotay D, and Wang P. “A simple and versatile cloud-screening method for MAX-DOAS retrievals.” *Atmos. Meas. Tech. Discuss.* 7, 5883-5920. (2014).
- González Abad, G., Liu, X., Chance, K., Wang, H., Kurosu, T. P., and Suleiman, R. “Updated SAO OMI formaldehyde retrieval.” *Atmos. Meas. Tech. Discuss.* 7, 1-31. (2014).
- Haagen-Smit A. “Chemistry and Physiology of Los Angeles Smog.” *Air Pollution*. Vol 44, No 6, 1342-1346. (1952).
- Hewson W, Barkley M, Gonzalez Abad G, Bosch H, Kurosu T, Spurr R, and Tilstra L. “Development and characterization of a state-of-the-art GOME-2 formaldehyde air-mass factor algorithm.” *Atmos. Meas. Tech.* 8, 4055-4074. (2015).
- Holmes C, Prather M, and Vinken G. “The climate impact of ship NO<sub>x</sub> emissions: an improved estimate accounting for plume chemistry.” *Atmos. Chem. Phys. Discuss.* 14, 3427-3458. (2014).
- Honninger G, von Friedeburg C, and Platt U. “Multi axis differential optical absorption spectroscopy.” *Atmospheric Chemistry and Physics*. 4 (2004) 231-254.
- Johansson M, Galle B, Yu T, Tang L, Chen D, Li H, Li J, and Zhang Y. “Quantification of total emission of air pollutants from Beijing using mobile mini-DOAS.” *Atmospheric Environment*. 42, 6926-6933 (2008).
- Johansson M, Rivera C, de Foy B, Lei W, Song J, Zhang Y, Galle B, and Molina L. “Mobile mini-DOAS measurement of the outflow of NO<sub>2</sub> and HCHO from Mexico City.” *Atmos. Chem. Phys.* 9, 5647-5653 (2009).
- Kim J, Kim S, Baek K, Wang L, Kurosu T, De Smedt I, Chance K, and Newchurch M. “Evaluation of satellite-derived HCHO using standard methods.” *Atmos. Chem. Phys. Discuss.* 11, 8003-8025. (2011).

- Kim S, Heckel A, Frost G, Richter A, Gleason J, Burrows J, McKeen S, Hsie E, Granier C, and Trainer M. "NO<sub>2</sub> columns in the western United States observed from space and simulated by a regional chemistry model and their implications for NO<sub>x</sub> emissions." *Journal of Geophysical Research*. Vol. 114, D11301 (2009).
- Kim S, McKeen S, Frost G, Lee S, Trainer M, Richter A, Angevine W, Atlas E, Bianco L, Boersma K, Brioude J, Burrows J, de Gouw J, Fried A, Gleason J, Hilboll A, Mellqvist J, Peischl J, Richter D, Rivera C, Ryerson T, te Lintel Hekkert S, Walega J, Warneke C, Weibring P, and Williams E. "Evaluations of NO<sub>x</sub> and highly reactive VOC emission inventories in Texas and their implications for ozone plume simulations during the Texas Air Quality Study 2006." *Atmos. Chem. Phys.* 11, 11361-11386 (2011).
- Lamsal L, Martin R, van Donkelaar A, Steinbacher M, Celarier E, Buscela E, Dunlea E, Pinto J. "Ground-level nitrogen dioxide concentrations inferred from the satellite-borne Ozone Monitoring Instrument." *Journal of Geophysical Research*. 113, D16308. (2008).
- Lee C, Kim Y, Lee H, and Choi B. "Chapter 3: MAX-DOAS Measurements of ClO, SO<sub>2</sub>, and NO<sub>2</sub> in the Mid-Latitude Coastal Boundary Layer and a Power Plant Plume." *Advanced Environmental Monitoring*. 37-49 (2008).
- Levelt P, van den Oord H, Dobber M, Mälkki A, Visser H, de Vries J, Stammes P, Lundell J, and Saari H. "The Ozone Monitoring Instrument." *IEEE Transactions on Geoscience and Remote Sensing*. Vol. 44, No. 5. (2006).
- Lin J. "Satellite constraint for emissions of nitrogen oxides from anthropogenic, lightning and soil sources over East China on a high-resolution grid." *Atmos. Chem. Phys.* 12, 2881-2898. (2012).
- Lonsdale C, Stevens R, Brock C, Makar P, Knipping E, and Pierce J. "The effect of coal-fire power-plant SO<sub>2</sub> and NO<sub>x</sub> control technology on aerosol nucleation in the source plumes." *Atmos. Chem. Physics*. 12, 11519-11531. (2012).
- Luhana L, Middleton D, and Sokhi R. *Processes and parameters influencing the oxidation of SO<sub>2</sub> and NO<sub>x</sub> in plumes*. (2007).



- Martin R, Fiore A, and Van Donkelaar A. "Space-bases diagnosis of surface ozone sensitivity to anthropogenic emissions." *Geophysical Research Letters*. 31, L06120. (2004a).
- Martin R, Parrish D, Ryerson T, Nicks D, Chance K, Kurosu T, Jacob D, Sturges E, Fried A, and Wert B. "Evaluation of GOME satellite measurements of tropospheric NO<sub>2</sub> and HCHO using regional data from aircraft campaigns in the southeastern United States." *Journal of Geophysical Research: Atmospheres*. 109, D24. (2004b).
- McIntosh C. "The fuel use and air emission consequences of shipping Great Lakes coal through the Soo Locks." *Transportation Research Part D*. 18, 117-121. (2013).
- Millet D, Jacob D, Turquety S, Hudman R, Wu S, Fried A, Walega J, Heikes B, Blake D, Singh H, Anderson B, and Clarke A. "Formaldehyde distribution over North America: Implications for satellite retrievals of formaldehyde columns and isoprene emissions." *Journal of Geophysical Research*. 111, D24S02. (2006).
- Olszyna K, Bailey E, Simonaitis R, and Meagher J. "O<sub>3</sub> and NO<sub>y</sub> relationships at a rural site." *Journal of Geophysical Research*. 99, D7, 14557-14563. (1994).
- Palmer P, Jacob D, Fiore A, Martin R, Chance K, and Kurosu T. "Mapping isoprene emissions over North America using formaldehyde column observations from space." *Journal of Geophysical Research*. 108, D6, 4180. (2003).
- Platt U and Stutz J. *Differential Optical Absorption Spectroscopy*. (2008).
- Prata A. "Measuring SO<sub>2</sub> ship emission with an ultra-violet imaging camera." *Atmos. Meas. Tech. Discuss*. 6, 9467-9511. (2013).
- Pyle DM and Mather TA. "Halogens in igneous processes and their fluxes to the atmosphere and oceans from volcanic activity: A review." *Chemical Geology*. 263 (2009) 110-121.
- Redling K, Elliott E, and Bain D. "Highway contributions to reactive nitrogen deposition: tracing the fate of vehicular NO<sub>x</sub> using stable isotopes and plant biomonitors." *Biogeochemistry*. 116:261-274. (2013).
- Russell AR, Valin LC, and Cohen RC. "Trends in OMI NO<sub>2</sub> observations over the United States: effects of emission control technology and the economic recession." *Atmos. Chem. Phys*. 12 (2012) 12197-12209.

- Sandstrom, T. "Respiratory effects of air pollutants: experimental studies in humans." *European Respiratory Journal*. 8(6): 976-995. (1995).
- Seinfeld JH and Pandis SN. *Atmospheric Chemistry and Physics*. John Wiley and Sons (2006).
- Singer B, Hodgson A, Hotchi T, and Kim J. "Passive measurement of nitrogen oxides to assess traffic-related pollutant exposure for the East Bay Children's Respiratory Health Study." *Atmospheric Environment*. Vol. 38, Iss. 3, Pg. 393-403. (2004).
- Tzannatos E. "Ship emissions and their externalities for Greece." *Atmospheric Environment*. 1-9. (2010).
- Wagner T, Ibrahim O, Shaiganfar R, and Platt U. "Mobile MAX-DOAS observations of tropospheric trace gases." *Atmos. Meas. Tech.* 3, 129-140 (2010).
- Washenfelder R, Trainer M, Frost G, Ryerson T, Atlas E, de Gouw J, Flocke F, Fried A, Holloway J, Parrish D, Peischl J, Richter D, Schauffler S, Walega J, Warnke C, Weibring P, and Zheng W. "Characterization of NO<sub>x</sub>, SO<sub>2</sub>, ethane, and propene from industrial emission sources in Houston, Texas." *Journal of Geophysical Research*. Vol. 115, D16311 (2010).
- Wu F, Xie P, Li A, Chan K, Hartl A, Wang Y, Si F, Zeng Y, Qin M, Xu J, Liu J, Liu W, Wenig M. "Observations of SO<sub>2</sub> and NO<sub>2</sub> by mobile DOAS in the Guangzhou Eastern Area during the Asian Games 2010." *Atmos. Meas. Tech. Discuss.* 6, 261-301 (2013).
- Homer, C.G., Dewitz, J.A., Yang, L., Jin, S., Danielson, P., Xian, G., Coulston, J., Herold, N.D., Wickham, J.D., and Megown, K. "Completion of the 2011 National Land Cover Database for the conterminous United States-Representing a decade of land cover change information." *Photogrammetric Engineering and Remote Sensing*, v. 81, no. 5, p. 345-354. (2015).
- Zavala M, Herndon S, Slott R, Dunlea E, Marr L, Shorter J, Zahniser M, Knighton W, Rogers T, Kolb C, Molina L, and Molina M. "Characterization of on-road vehicle emissions in the Mexico City Metropolitan Area using a mobile laboratory in chase and fleet average measurement modes during the MCMA-2003 field campaign." *Atmos. Chem. Phys.* 6, 5129-5142. (2006).

- Zhang Y, Wang H, Somesfalean G, Wang Z, Lou X, Wu S, Zhang Z, and Qin Y. "Broadband UV spectroscopy system used for monitoring of SO<sub>2</sub> and NO emissions from thermal power plants." *Atmospheric Environment*. 44, 4266-4271 (2010).
- Zhou W, Cohan D, Pinder R, Neuman J, Holloway J, Peischl J, Ryerson T, Nowak J, Flocke F, and Zheng W. "Observation and modeling of the evolution of Texas power plant plumes." *Atmos. Chem. Phys.* 12, 455-468 (2012).
- Zhu L, Jacob D, Mickley L, Marais E, Cohan D, Yoshida Y, Duncan B, Gonzalez Abad G, Chance K. "Anthropogenic emissions of highly reactive volatile organic compounds in eastern Texas inferred from oversampling of satellite (OMI) measurements of HCHO columns." *Environ. Res. Lett.* 9, 114004. (2014).